

1 Space for WHAM: a multi-region, multi-stock generalization of the
2 Woods Hole Assessment Model with an application to black sea
3 bass

4 Timothy J. Miller¹ Kiersten L. Curti Alexander C. Hansell

5 16 May, 2025

6 ¹timothy.j.miller@noaa.gov, Northeast Fisheries Science Center, National Marine Fisheries Service, 166
7 Water Street, Woods Hole, MA 02543, USA

keywords: stock assessment, state-space, multi-stock, multi-region, age-structured, black sea bass

Abstract

The Woods Hole Assessment Model is a general state-space age-structured assessment model that is used to assess and manage many stocks in the Northeast US. We first describe an extension of the model allowing any number of stocks (or stock components) and regions with movement among regions as well as seasonal variation in stock and fleet dynamics. Movement rates can be functions of time- and age-varying random effects and environmental covariates. We then illustrate the model by applying it to data for the northern and southern components of the Northeast United States black sea bass stock and evaluate alternative hypotheses of bottom temperature and time-varying random effects on recruitment and natural mortality. We show strong evidence for temperature effects on recruitment, primarily for the northern stock component, and no evidence for including random effects or temperature effects on age 1 natural mortality.

Introduction

State-space age-structured stock assessment models can be used to estimate time and age-varying population attributes as random effects using maximum marginal likelihood or Bayesian fitting procedures (Nielsen and Berg 2014; Cadigan 2016; Miller et al. 2016b). This estimation approach is considered an essential feature of gold-standard assessment models that we use in tactical management of commercially important fish stocks (Punt et al. 2020). The State-space Assessment Model (SAM, Nielsen and Berg 2014) continues to be developed and remains widely used within the International Council for the Exploration of the Sea (ICES) to assess European fish stocks. Various state-space models are being used to manage cod and plaice stocks in the waters of Eastern Canada (Perreault et al. 2020; Varkey et al. 2022) and to the south, the Woods Hole Assessment Model (WHAM, Miller and Stock 2020; Stock and Miller 2021) is now used to assess many fish stocks in the Northwest Atlantic Ocean (NEFSC 2022a, 2022b; NEFSC 2024a).

WHAM is an R package developed and maintained by scientists at NOAA’s Northeast Fisheries Science Center (<https://timjmiller.github.io/wham>). WHAM can be configured to fit a wide range of age-structured models from traditional statistical catch-at-age models without any random effects to models with several time and age varying process errors and effects of environmental covariates on various population parameters. Like SAM, WHAM models are built using the Template Model Builder package (TMB, Kristensen et al. 2016) which provides a computationally efficient means of fitting an extremely wide class of models with random effects. WHAM has undergone active development since its creation and includes random effects options for recruitment, inter-annual transitions of numbers at age (hereafter referred to as “apparent survival”), fishery and index selectivity, natural mortality, and catchability.

However, WHAM has only allowed one stock and a single region and without seasonal changes in stock dynamics. Using such models for stocks that have subcomponents with varying seasonal movement can provide incorrect inferences and poor management advice (Ying et al. 2011; Cao et al. 2014; Bosley et al. 2022). Furthermore, the ability to account for spatial structure and model multiple stocks are also important features of leading-edge assessment modeling frameworks (Punt et al. 2020). We describe here the implementation of these features and other extensions since Stock and Miller (2021) in WHAM version 2.0. Many of these new configuration options can also be useful when modeling a single stock and region.

We developed this extension of WHAM in concert with a research track assessment process for black sea bass (*Centropomus striata*) (NEFSC 2023). Black sea bass is a high profile stock in the Northeast U.S. and important to both commercial fishing fleets and recreational anglers. Black sea bass are targeted from Maine to North Carolina in both state and federal waters. Past stock assessments have estimated that the

stock is healthy (not overfished and overfishing not occurring). Previous assessments assumed two stock components (north and south), each assessed with a separate statistical catch at age model with results subsequently combined to inform management, but these assessments have exhibited strong retrospective patterns. The stock was split into two regional components to account for spatial dynamics and improve model diagnostics (ASMFC 2016). Additionally, black sea bass have complex spatial dynamics and make seasonal migrations, moving inshore in the spring and offshore in the fall (Moser and Shepherd 2009). Black sea bass distribution has been linked to warming waters on the northwest shelf (Bell et al. 2015) and it is hypothesized that the distribution and productivity of the black sea bass stock is especially susceptible to long-term changes in temperature causing increases in abundance further north (Hare et al. 2016). Thus, a focus of the black sea bass research track assessment was to develop an assessment platform that could capture multiple stock components, complex seasonal movement, and explore environmental drivers of population dynamics (NEFSC 2023). We denote the fish in the north as separate stock components rather than stocks because both components are managed as a single stock, but recognizing differences in migration between fish originating in the two areas.

To illustrate the usage of WHAM 2.0 we apply it to the two stock components of black sea bass off the coast of the Northeast United States (NEUS) using most of the model assumptions that were accepted during the peer-review process. However, here we evaluate evidence for alternative hypotheses of temporal variation and effects specifically of bottom temperature on recruitment and natural mortality of age 1 individuals.

When modeling multiple stock components occurring in different regions, further dimensionality is added to the class of possible equilibrium reference points (e.g., Kapur et al. 2021). Short term projections are also an important part of the management process and the separation of observation and process errors in state-space models allows uncertainty in projected attributes such as recruitment and spawning stock biomass (SSB) without external simulation exercises. Finally, the inclusion of explicit effects of environmental covariates in the model also requires assumptions on how they are treated in projections and reference points. We demonstrate some of the options of WHAM version 2.0 to provide biological reference points and short-term projections.

Methods

WHAM description

Many of the options and equations of WHAM version 2.0 are the same as those in Stock and Miller (2021), so we will only describe extensions and differences that have occurred since their first description of WHAM. The new version of WHAM can model multiple stocks each with their own movement, harvest, and natural mortality. Much of the description below is for a specific stock s , but, for simplicity, this subscript is implicit except when necessary.

The probability transition matrix

Because individuals may be alive in one of several regions or harvested in one of several fleets, it is helpful to consider these as distinct categories or states and treat the number of individuals occurring in each category over time as a multi-state model. Approaches to modeling transitions among these states may treat time discretely (e.g., Arnason 1972; Schwarz et al. 1993) or continuously (e.g., Hearn et al. 1987; Commenges 1999; Andersen and Keiding 2002). We can define a probability transition matrix (PTM) that describes the probability of individuals occurring in different states at the end of a time interval with duration δ (columns), conditional on being in each of those states at the beginning of the interval (rows). For fish populations, these states would be defined as being alive in a particular region or deceased due to fishing from a particular fleet or natural mortality. The time interval i with duration δ_i would be a season and the PTMs would be uniquely defined for each stock by year y , age a , and season i on January 1. Each row and column of the PTM correspond to one of the states: alive in region r , dead in fleet f , or dead from natural causes. The probabilities in each row sum to unity (must be in one of the states) and assume an individual is in the state that corresponds to that row at the beginning of the interval. Given n_R regions and n_F fleets, the square PTM ($n_R + n_F + 1$ rows and columns) as a function of sub-matrices is

$$\mathbf{P}_{y,a,i} = \begin{bmatrix} \mathbf{O}_{y,a,i} & \mathbf{H}_{y,a,i} & \mathbf{D}_{y,a,i} \\ 0 & \mathbf{I}_H & 0 \\ 0 & 0 & 1 \end{bmatrix} \quad (1)$$

99 where

$$\mathbf{O}_{y,a,i} = \begin{bmatrix} O_{y,a,i}(1,1) & \cdots & O_{y,a,i}(1,n_R) \\ \vdots & \ddots & \vdots \\ O_{y,a,i}(n_R,1) & \cdots & O_{y,a,i}(n_R,n_R) \end{bmatrix}$$

100 is the $n_R \times n_R$ matrix defining survival and occurring in each region at the end of the interval,

$$\mathbf{H}_{y,a,i} = \begin{bmatrix} H_{y,a,i}(1,1) & \cdots & H_{y,a,i}(1,n_F) \\ \vdots & \ddots & \vdots \\ H_{y,a,i}(n_R,1) & \cdots & H_{y,a,i}(n_R,n_F) \end{bmatrix}$$

101 is the $n_R \times n_F$ matrix defining probabilities of being captured in each fleet during the interval, and $\mathbf{D}_{y,a,i}$ is
 102 the $n_R \times 1$ matrix of probabilities of dying due to natural mortality during the interval. We have the $n_F \times n_F$
 103 identity matrix \mathbf{I}_H for the states of capture by each fleet and a 1 for the natural mortality state because
 104 the probabilities of being in one of the mortality states given starting the interval in that state is unity (no
 105 zombies allowed).

106 WHAM uses these PTMs to model abundance proportions in each state rather than true probabilities where
 107 numbers in each state would have a multinomial distribution as in a model for tagging data where fates
 108 of individual tagged fish are assumed independent. The PTMs determine the expected numbers 1) in each
 109 state on January 1 of year $t + 1$ at age $a + 1$ given the abundances at age a on January 1 of year t , 2)
 110 captured over the year in each fleet, 3) available to each index, and 4) alive at the time and in the region
 111 where spawning occurs.

112 Single region PTMs

113 When there is only one region,

$$\mathbf{P}_{y,a,i} = \begin{bmatrix} S_{y,a,i} & \mathbf{H}_{y,a,i} & D_{y,a,i} \\ 0 & \mathbf{I}_H & 0 \\ 0 & 0 & 1 \end{bmatrix} \quad (2)$$

114 where $S_{y,a,i} = e^{-Z_{y,a,i}\delta_i}$, $\mathbf{H}_{y,a,i}$ is a $1 \times n_F$ matrix with elements for each fleet f : $\frac{F_{y,a,i,f}}{Z_{y,a,i}} (1 - e^{-Z_{y,a,i}\delta_i})$,
 115 $D_{y,a,i} = \frac{M_{y,a}}{Z_{y,a,i}} (1 - e^{-Z_{y,a,i}\delta_i})$, and $Z_{y,a,i} = M_{y,a} + \sum_{f=1}^{n_F} F_{y,a,i,f}$ is the total mortality rate.

Multi-region PTMs

When there is more than one region, WHAM can model survival and movement as processes occurring sequentially or simultaneously. The sequential assumption is used widely in spatially explicit models (e.g., Stock Synthesis, Methot and Wetzel 2013). Under the sequential assumption, survival and death occur over the interval and movement among regions occurs instantly at either the beginning or the end of the interval. WHAM is configured to have movement occur after survival:

$$\mathbf{O}_{y,a,i} = \mathbf{S}_{y,a,i} \boldsymbol{\mu}_{y,a,i}$$

where $\mathbf{S}_{y,a,i}$ is a $n_R \times n_R$ diagonal matrix of proportions surviving in each region (given they start in that region)

$$\mathbf{S}_{y,a,i} = \begin{bmatrix} e^{-Z_{y,a,i,1}\delta_i} & 0 & \dots & 0 \\ 0 & e^{-Z_{y,a,i,2}\delta_i} & \dots & 0 \\ \vdots & \vdots & \ddots & \vdots \\ 0 & \dots & 0 & e^{-Z_{y,a,i,n_R}\delta_i} \end{bmatrix}$$

and $\boldsymbol{\mu}_{y,a,i}$ is a $n_R \times n_R$ matrix of probabilities of moving from one region to another or staying in the region they occurred at the beginning of the interval:

$$\boldsymbol{\mu}_{y,a,i} = \begin{bmatrix} 1 - \sum_{r' \neq 1} \mu_{1 \rightarrow r', y, a, i} & \mu_{1 \rightarrow 2, y, a, i} & \dots & \mu_{1 \rightarrow R, y, a, i} \\ \mu_{2 \rightarrow 1, y, a, i} & 1 - \sum_{r' \neq 2} \mu_{2 \rightarrow r', y, a, i} & \dots & \mu_{2 \rightarrow R, y, a, i} \\ \vdots & \vdots & \ddots & \vdots \\ \mu_{R \rightarrow 1, y, a, i} & \dots & \mu_{R \rightarrow R-1, y, a, i} & 1 - \sum_{r' \neq R} \mu_{R \rightarrow r', y, a, i} \end{bmatrix}$$

WHAM assumes each fleet f can harvest in only one region (r_f) during specified seasons. So, for each fleet f , row r_f and column f of $\mathbf{H}_{y,a,i}$ will be $F_{y,a,i,f} (1 - e^{-Z_{y,a,i,r}\delta_i}) / Z_{y,a,i,r}$ when fleet f is harvesting during the interval i and all other elements will be zero. Row r of the single-column matrix $\mathbf{D}_{y,a,i}$ is $M_{y,a,r} (1 - e^{-Z_{y,a,i,r}\delta_i}) / Z_{y,a,i,r}$. For details defining PTMs with movement and mortality occurring simultaneously see Appendix B.

Seasonality

Seasonality can be configured to accommodate characteristics of spawning, movement, and fleet-specific behavior. The annual time step can be divided into K seasons and the interval duration δ_i for each season

134 i does not need to be equal to any other seasonal interval. Under the Markov assumption the PTMs for
 135 each consecutive interval are independent and the PTM of surviving and moving and dying over K intervals
 136 $1, \dots, K$ (i.e., the entire year) is just the product of the PTMs for each interval:

$$\mathbf{P}_{y,a}(\delta_1, \dots, \delta_K) = \prod_{i=1}^K \mathbf{P}_{y,a,i}(\delta_i).$$

137 For a stock spawning at some fraction of the year $0 < t_s < 1$ in interval $i \in \{1, \dots, K\}$, the fraction of time
 138 in the interval is

$$\delta_{s,i} = t_s - \sum_{j=0}^{i-1} \delta_j$$

139 (where $\delta_0 = 0$) and the PTM defining the proportions in each state at time t_s for age a is

$$\mathbf{P}_{y,a}(\delta_1, \dots, \delta_{i-1}, \delta_{s,i}) = \mathbf{P}_{y,a}(t_s) = \left[\prod_{j=0}^{i-1} \mathbf{P}_{y,a,j}(\delta_j) \right] \mathbf{P}_{y,a,i}(\delta_{s,i}) \quad (3)$$

140 where $\mathbf{P}_{y,a,0}$ is an identity matrix. Similarly, for an index m occurring at fraction of the year t_m in interval
 141 i the proportions in each state at the time of the observation is

$$\mathbf{P}_{y,a}(\delta_1, \dots, \delta_{i-1}, \delta_{m,i}) = \mathbf{P}_{y,a}(t_m) = \left[\prod_{j=0}^{i-1} \mathbf{P}_{y,a,i}(\delta_j) \right] \mathbf{P}_{y,a,i}(\delta_{m,i}). \quad (4)$$

142 Numbers at age

143 When there are n_R regions and n_F fleets, the vector of abundance in each state at age $a > 1$ on January 1
 144 is $\mathbf{N}_{y,a} = (\mathbf{N}_{O,y,a}^T, \mathbf{0}^T)^T$ where $\mathbf{N}_{O,y,a} = (N_{y,a,1}, \dots, N_{y,a,n_R})^T$ is the number in the states corresponding to
 145 being alive in each region and $\mathbf{0}$ is a vector $(n_F + 1)$ for the numbers captured in each fleet and dead from
 146 natural mortality because no age a fish have died yet on January 1.

147 Each stock s is assumed to spawn and recruit in one region r_s . So for age $a = 1$, $\mathbf{N}_{O,y,1}$ is 0 except for
 148 row $r = r_s$. Options for configuring recruitment $(N_{y,1,r_s})$ for each stock are the same as previous versions of
 149 WHAM (Miller and Stock 2020). If recruitment is assumed to be a function of SSB, it is only the spawning
 150 population in region r_s at the time of spawning that constitutes the SSB in the stock-recruit function.
 151 However, models can configure individuals to occur in other regions at the time of spawning. Aside from
 152 treating recruitment as a random walk, the general model for annual recruitment as random effects is

$$\log(N_{y,1,r_s}) | \text{SSB}_{y-1,r_s} = f(\text{SSB}_{y-1,r_s}) + \varepsilon_{y,1,r_s}$$

where

$$\text{SSB}_{y,r_s} = \sum_{a=1}^A w_{y,a} \text{mat}_{y,a} \mathbf{O}_{y,a,r_s}^T(t_s) \mathbf{N}_{O,y,a}$$

and $w_{y,a}$ and $\text{mat}_{y,a}$ are the stock-specific mean weight at age of spawning individuals and maturity at age, respectively, and $\mathbf{O}_{y,a,r_s}(t_s)$ are the probabilities of surviving and occurring in region r_s at time t_s given being alive in each region at the start of the year (the r_s column of the upper-left submatrix of Eq. 3).

As in previous versions of WHAM, the apparent survival (and movement) from one year to another after recruitment can be treated deterministically or as functions of random effects. The predicted numbers at age a in year y for a given stock are vector analogs ($\mathbf{N}_{O,y,a}$) of the equations for numbers at age in the standard WHAM model (Stock and Miller 2021). For ages $a = 2, \dots, A - 1$, where A is the plus group, the expected number alive in each region at the beginning of the following year and next age class age can be obtained from the first n_R elements of the vector

$$\mathbf{P}_{y-1,a-1}^T \mathbf{N}_{y-1,a-1}.$$

The numbers alive in each region can also be modeled more simply using the sub-matrix $\mathbf{O}_{y,a}$. The general model for the vector of abundance at age in year y at age a given the vector in year $y - 1$ at age $a - 1$ is

$$\log(\mathbf{N}_{O,y,a}) | \mathbf{N}_{O,y-1,a-1} = \log(\mathbf{O}_{y-1,a-1}^T \mathbf{N}_{O,y-1,a-1}) + \boldsymbol{\varepsilon}_{y,a}$$

for ages $a = 2, \dots, A - 1$, and for the plus group

$$\log(\mathbf{N}_{O,y,A}) | \mathbf{N}_{O,y-1,A-1}, \mathbf{N}_{O,y-1,A} = \log(\mathbf{O}_{y-1,A-1}^T \mathbf{N}_{O,y-1,A-1} + \mathbf{O}_{y-1,A}^T \mathbf{N}_{O,y-1,A}) + \boldsymbol{\varepsilon}_{y,A}$$

where $\boldsymbol{\varepsilon}_{y,a}$ is the vector of region-specific errors for a given stock, which are independent across stocks and regions, but the same correlation structures as previous versions are possible across ages and years for a given stock and region.

When there is autocorrelation with age, WHAM now assumes this applies only to ages $a > 1$ by default so that recruitment random effects are independent of those for the apparent survival of older age classes. So the general covariance structure for a given stock at ages $a > 1$ in region r is that of a two-dimensional

173 first-order autoregressive (2DAR1) process

$$Cov(\varepsilon_{y,a,r}, \varepsilon_{y',a',r}) = \frac{\rho_{N,\text{age},r}^{|a-a'|} \rho_{N,\text{year},r}^{|y-y'|} \sigma_{N,a,r} \sigma_{N,a',r}}{(1 - \rho_{N,\text{age},r}^2)(1 - \rho_{N,\text{year},r}^2)}$$

174 and that for age 1 is just AR1 across years

$$Cov(\varepsilon_{y,1}, \varepsilon_{y',1}) = \frac{\rho_{N,1,\text{year}}^{|y-y'|} \sigma_{N,1}^2}{1 - \rho_{N,1,\text{year}}^2}.$$

175 When the annual changes in abundance at age are treated deterministically, $\varepsilon_{y,a} = 0$. Since recruitment for
 176 a given stock currently only occurs in one region r_s there is only a single vector of time-varying recruitment
 177 random effects for each stock.

178 Initial numbers at age

179 Initial numbers at age for each stock and region can be treated as age-specific fixed effects or with an equi-
 180 librium assumption as in previous versions of WHAM. For the equilibrium option there are two parameters
 181 for each stock: the stock-specific fully-selected fishing mortality rate $\log \tilde{F}$ and the recruitment in year 1
 182 $\log N_{1,1,r_s}$. A stock-specific equilibrium fishing mortality at age by fleet $\tilde{F}_{a,f}$ is the product of \tilde{F} and the
 183 selectivity across fleets in the first year

$$\text{sel}_{1,a,f} = \frac{F_{1,a,f}}{\max_a \sum_{f=1}^{n_F} F_{1,a,f}}.$$

184 We use $\tilde{F}_{a,f}$ to define an equilibrium abundance per recruit by region at age a conditional on recruiting to
 185 each region

$$\tilde{\mathbf{O}}_a = \begin{cases} \prod_{j=0}^{a-1} \mathbf{O}_j & 1 \leq a < A \\ \left[\prod_{j=0}^{a-1} \mathbf{O}_j \right] (\mathbf{I} - \mathbf{O}_A)^{-1} & a = A \end{cases} \quad (5)$$

186 where \mathbf{O}_j is the equilibrium probability of surviving age a and occurring in each region and $\mathbf{O}_0 = \mathbf{I}$. Natural
 187 mortality and movement rates in the first year of the model are also used in Eq. 5. For the plus group $a = A$,
 188 $(\mathbf{I} - \mathbf{O}_A)^{-1}$ is a “fundamental matrix” derived using the matrix version of the geometric series (Kemeny and
 189 Snell 1960). Recall that recruitment for stock s only occurs in region r_s so, the equilibrium initial numbers
 190 at age a by region are

$$\mathbf{N}_{O,1,a} = \tilde{\mathbf{O}}_a^T \mathbf{N}_{O,1,1}.$$

191 Initial abundance at age can also be estimated as random effects as described in Appendix B.

192 Parametizing movement

193 For each season, there are at most $n_R - 1$ parameters determining movement for a given stock among regions
 194 given starting the season in region r in either the sequential or simultaneous configurations. Movement
 195 parameters are estimated on a transformed scale via a link function $g(\cdot)$. If survival and movement occur
 196 simultaneously, the parameters are estimated with a log link function and if they are separable, an additive
 197 logit link function (like a multinomial regression) is used. On the transformed scale, the general model for
 198 the movement parameter from region r to r' in season i and year y for individuals of age a is a linear function
 199 of an intercept or mean parameter ($\theta_{r \rightarrow r', i}$) and both random and environmental effects:

$$g(\mu_{r \rightarrow r', y, a, i}) = \theta_{r \rightarrow r', i} + \varepsilon_{r \rightarrow r', y, a, i} + \sum_{k=1}^{n_E} \beta_{r \rightarrow r', a, i, k} E_{k, y}.$$

200 The random effects $\varepsilon_{r \rightarrow r', y, a, i}$ are season-, and region-to-region-specific and modeled most generally as
 201 2DAR1 random effects with age and(or) year where the covariance is

$$Cov(\varepsilon_{r \rightarrow r', y, a, i}, \varepsilon_{r \rightarrow r', y', a', i}) = \frac{\rho_{r \rightarrow r', \text{age}, i}^{|a-a'|} \rho_{r \rightarrow r', \text{year}, i}^{|y-y'|} \sigma_{r \rightarrow r', i}^2}{\left(1 - \rho_{r \rightarrow r', \text{age}, i}^2\right) \left(1 - \rho_{r \rightarrow r', \text{year}, i}^2\right)}$$

202 similar to how WHAM models variation in survival, natural mortality, and selectivity. Effects of covariate
 203 E_k can be age-, season-, and region-to-region-specific $\beta_{r \rightarrow r', a, i, k}$ and the same orthogonal polynomial options
 204 in the previous versions of WHAM for effects on recruitment and natural mortality are available.

205 There is currently no likelihood component for tagging data. Therefore, movement parameters would usually
 206 either need to be fixed or assumed to have some prior distribution, possibly based on external parameter
 207 estimates. WHAM includes prior distributions for the season and region-to-region specific (mean) movement
 208 parameters and treats them as random effects with the mean defined by the initial value of the fixed effect
 209 counterpart and standard deviation

$$\gamma_{r \rightarrow r', i} \sim N(\theta_{r \rightarrow r', i}, \sigma_{r \rightarrow r', i}^2).$$

210 When priors are used, the movement is defined instead as

$$g(\mu_{r \rightarrow r', y, a, i}) = \gamma_{r \rightarrow r', i} + \varepsilon_{r \rightarrow r', y, a, i} + \sum_{k=1}^{n_E} \beta_{r \rightarrow r', a, i, k} E_{k, y}.$$

211 Natural mortality

212 When treated as constant parameters, natural mortality rates may be stock-, region-, and age-specific, but
 213 currently are constant across seasons. When random effects are used, the same 2DAR1 structure with age
 214 and year as described by Stock and Miller (2021) can be configured for a given stock and region and any
 215 environmental covariate effects can be stock-, region-, and age-specific. See Appendix B for details.

216 Catch observations

217 The log-normal distributional assumption for aggregate catch observations is the same as Stock and Miller
 218 (2021), but the predicted catch is now a function of catch from each stock starting the year in each region
 219 and any seasonal movement. For a given stock and age, the vector of numbers captured by each fleet over
 220 the year are

$$\hat{\mathbf{N}}_{H,s,y,a} = \mathbf{H}_{s,y,a}^T \mathbf{N}_{O,s,y,a}$$

221 (recall each fleet can harvest in only one region as described above). The vector of predicted numbers caught
 222 by each fleet across stocks is

$$\hat{\mathbf{N}}_{H,y,a} = \sum_{s=1}^{n_S} \hat{\mathbf{N}}_{H,s,y,a}$$

223 and the vector of predicted aggregate catch by each fleet at age a is

$$\hat{\mathbf{C}}_{y,a} = \text{diag}(\mathbf{c}_{y,a}) \hat{\mathbf{N}}_{H,y,a}$$

224 where $\mathbf{c}_{y,a}$ is the vector of mean individual weight at age a for each fleet and the aggregate catch by fleet is

$$\hat{\mathbf{C}}_y = \sum_{a=1}^A \hat{\mathbf{C}}_{y,a}.$$

225 The log-aggregate catch observations for fleet f are normally distributed

$$\log C_{y,f} \sim \mathcal{N}\left(\log \hat{C}_{y,f}, \sigma_{y,f}^2\right).$$

226 The predicted numbers caught for each fleet f (row f of $\hat{\mathbf{N}}_{H,y,a}$) are used to make predicted age composition
 227 observations as described by Stock and Miller (2021). Since then, three additional likelihood options for
 228 age composition observations have been added: a logistic-normal with AR(1) correlation structure (Francis
 229 2014), the alternative Dirichlet-multinomial parameterization described by Thorson et al. (2017), and the

230 multivariate Tweedie (Thorson et al. 2023).

231 Index observations

232 Like fishing fleets, an index m can observe the population in a single region r_m at fraction of the year t_m ,
 233 the predicted abundance at t_m in region r_m is

$$\hat{N}_{s,y,a,m} = \mathbf{O}_{s,y,a,r_m}^T(t_m) \mathbf{N}_{O,s,y,a}$$

234 where $\mathbf{O}_{s,y,a,r_m}(t_m)$, the r_m column of the upper-left submatrix of Eq. 4, are the probabilities of surviving
 235 and occurring in region r_m at time t_m given being alive in each region at the start of the year. The predicted
 236 index at age is

$$\hat{I}_{m,y,a} = q_{m,y} \text{sel}_{m,y,a} w_{m,y,a} \sum_{s=1}^{n_S} \hat{N}_{s,y,a,m}$$

237 where $q_{m,y}$ is the catchability of the index in year y , $\text{sel}_{m,y,a}$ is the selectivity and $w_{m,y,a}$ is the average
 238 weight of individuals at age a if the index is quantified in biomass and $w_{m,y,a} = 1$ if the index is quantified
 239 in numbers. Predicted age composition observations are functions of $\hat{I}_{m,y,a}$ as described by Stock and Miller
 240 (2021) and the likelihood options are the same as those for catch explained above. See Appendix B for
 241 options to model temporal variation in catchability.

242 Reference points

243 Currently a single fishing mortality reference point \tilde{F} is estimated across stocks and regions and the fleet-
 244 and age-specific reference point is $\tilde{F}_{f,a} = \tilde{F} \text{sel}_{f,a}$. Selectivity is determined across fleets and ages as in the
 245 equilibrium assumption for initial abundance at age except here it is a function of average F at age over a
 246 user-defined set of years

$$\text{sel}_{a,f} = \frac{\bar{F}_{a,f}}{\max_a \sum_{f=1}^{n_F} \bar{F}_{a,f}} \quad (6)$$

247 The equilibrium spawning stock biomass per recruit for a given stock in region r_s is defined as

$$\phi(\tilde{F}) = \sum_{a=1}^A \tilde{\mathbf{O}}_{a,r_s,\cdot} \mathbf{O}_{a,\cdot,r_s}(t_s) w_a m_a \quad (7)$$

248 where w_a and m_a are the mean individual weight and probability of maturity at age a , $\tilde{\mathbf{O}}_a$ are as described
 249 in Eq. 5, and $\mathbf{O}_a(t_s)$ is the $n_R \times n_R$ upper-left sub-matrix of eq. 3 with the probabilities of surviving and
 250 occurring in each region r' at age $a + t_s$ given starting in region r at age a . The further subscripts r_s, \cdot

and \cdot, r_s indicate row or column r_s , respectively. Using these rows and columns is required because of the assumption that spawning and recruitment only occur in region r_s .

The equilibrium spawning biomass per recruit (eq. 7) is conditional on the region of recruitment r_s . The equilibrium recruitment depends on the stock dynamics. WHAM currently only allows complete spawning region fidelity so that a stock only spawns and recruits in a single region. Therefore, the equilibrium vector of numbers at age 1 for each state, $\tilde{\mathbf{N}}_1$, will only be nonzero in the row corresponding to the spawning region (r_s). The matrices of probabilities of surviving and occurring in each region, $\tilde{\mathbf{O}}_{s,a}$ and $\mathbf{O}_{s,a}(t_s)$, are functions of the fishing mortality rates for fleets in each region $\tilde{F}_{f,a}$.

The matrix of equilibrium yield per recruit by region and fleet as a function of \tilde{F} is calculated as

$$\tilde{\nu}(\tilde{F}) = \sum_{a=1}^A \tilde{\mathbf{O}}_{a,r_s,\cdot} \mathbf{H}_a \mathbf{c}_{s,a} \quad (8)$$

where \mathbf{c}_a is the vector of mean individual weight at age for each fleet, and $\mathbf{H}_{s,a}$ is the submatrix of the probabilities of being captured in each fleet over the interval from a to $a + 1$, defined in eq. 1.

As in previous versions of the WHAM package, reference points for prevailing conditions, average all of the inputs to the spawning biomass and yield per recruit calculations (weight, maturity, natural mortality, and movement) over a set of user-specified years as shown in eq. 6 for selectivity (e.g., last 5 years of the model).

For $X\%$ SPR-based reference points, we use a Newton method and iterate for steps $j = 1, \dots, 10$

$$\log \tilde{F}^j = \log \tilde{F}^{j-1} - \frac{h(\log \tilde{F}^{j-1})}{h^{(1)}(\log \tilde{F}^{j-1})} \quad (9)$$

where $h(\log F)$ is the difference between the weighted sums of spawning biomass per recruit at F and $X\%$ of unfished spawning biomass per recruit across stocks:

$$h(\log F) = \sum_{s=1}^{n_s} \lambda_s \left[\phi_s(F = e^{\log F}) - \frac{X}{100} \phi_s(F = 0) \right]. \quad (10)$$

where $\phi_s(F = 0)$ is the equilibrium unfished spawning biomass per recruit. $h^{(1)}(\log F)$ is the derivative of h with respect to $\log F$, and the weights to use for each stock λ_s can be specified by the user or relative to the average of recruitment for each stock over the same years the user defines to calculate “static” equilibrium spawning biomass and yield.

When a Beverton-Holt or Ricker stock recruit relationship is assumed, an analogous Newton method is used to find $\log F$ that maximizes yield for MSY-based reference points, which are also a functions of the

equilibrium yield per recruit (Eq. 8) and equilibrium recruitment. The function $h(\log F)$ and $h^{(1)}(\log F)$ in Eq. 9 are the first and second derivatives of the sum of the stock-specific equilibrium yields with respect to $\log F$ (analogous to that described by Miller et al. 2016b).

Projections

The projection options are generally the same as those for previous versions of WHAM (Miller and Stock 2020). When there is movement of any stocks, the user has the option to project and use any random effects for time-varying movement or use the average over user specified years, analogous to how natural mortality can be treated in the projection period. The projection of any environmental covariates has been revised to better include error in the estimated latent covariate in any effects on the population in projection years. Users can also specify a catch or fully-selected fishing mortality in each projection year and they can be fleet-specific.

Application to black sea bass

Black sea bass are a temperate reef fish in the western Atlantic Ocean ranging the entire east coast of the United States. Fish north of Cape Hatteras, NC, are considered to comprise a single NEUS stock unit, but individual populations exhibit spawning site fidelity (Able and Stanton Hales, Jr. 1997; Fabrizio et al. 2013). Fish in this northern stock component perform seasonal migrations out on the continental shelf in the fall and back to their inshore spawning areas during the spring (Musick and Mercer 1977). Analyses of tagging studies have demonstrated that the extent of seasonal migration varies along the coast such that fish from populations off of southern New England and further north move offshore and as far south as the coasts of Virginia and North Carolina, whereas fish in the southern portion of the stock range generally move shorter distances between inshore and offshore areas of similar latitude (Moser and Shepherd 2009).

Prior to its 2023 peer-reviewed assessment, the NEUS black sea bass stock was assessed using the Age-Structured Assessment Program (ASAP) model (Legault and Restrepo 1999), a single-stock and -region statistical catch-at-age model that estimates all model parameters as fixed effects. Northern and southern components of the NEUS black sea bass stock ascribed to regions divided by the Hudson Canyon were separately modeled in ASAP (Figure 1). Results from the separate ASAP models were combined for a unit-stock assessment. The ASAP-based assessments exhibited strong retrospective patterns (Mohn 1999), and exploring alternative modeling approaches for the northern and southern stock components has been a high priority for management.

Leading up to the 2023 peer-reviewed assessment, a working group (hereafter referred to as “Working Group”) composed of scientists from federal, state, and academic institutions determined an optimal data and model configuration for the black sea bass stock using the multi-stock and multi-region extension of WHAM described above (NEFSC 2023). This assessment included the two regions and two stock components and investigated inclusion of hypothesized environmental drivers that were prioritized research recommendations from previous black sea bass assessments. Below we describe the assumptions and configuration of the assessment model as determined by the Working Group as well as the alternative assumptions for recruitment and natural mortality in the models we fit to evaluate alternative hypotheses of bottom temperature effects on black sea bass.

Basic structure

The first year being modeled for the population is 1989 and the fishery and index data used in the model span from 1989 to 2021. The north and south stock components are modeled as separate populations that spawn and recruit in respective regions and there are eight age classes with the last being a plus group ($a \in \{1, \dots, 8+\}$). We have observations for each of four total fishing fleets, where two fishing fleets (recreational and commercial) operate in each region.

There are 11 “seasonal” intervals within each calendar year: five monthly time intervals from Jan 1 to May 31, a spawning season from June 1 to July 31, and five monthly intervals from August 1 to December 31. The southern stock component is assumed to never move to the northern region. For the northern component, a proportion $\mu_{N \rightarrow S}$ can move to the southern region each month during the last five months of the year, but no movement is allowed from the south to the north during this period (Figure 2). During the first four intervals of the year a proportion $\mu_{S \rightarrow N}$ of the northern component individuals in the south can move back to the north, but no movement from the north to south is allowed during this period. In the fifth interval (May), all northern component individuals remaining in the south are assumed to move back to the north for the subsequent spawning period. Survival and movement occur sequentially in each interval and each of the two movement proportions are assumed constant across intervals, ages, and years.

The two monthly movement matrices are

$$\mu_1 = \begin{bmatrix} 1 - \mu_{N \rightarrow S} & \mu_{N \rightarrow S} \\ 0 & 1 \end{bmatrix}$$

for the portion of the year after spawning and

$$\mu_2 = \begin{bmatrix} 1 & 0 \\ \mu_{S \rightarrow N} & 1 - \mu_{S \rightarrow N} \end{bmatrix}$$

for the portion of the year before spawning. As noted in the description of the general WHAM model, tagging data are not yet allowed. However, the Working Group also fit a Stock Synthesis model (Methot and Wetzel 2013) which included tagging data and provided estimated movement rate parameters and standard errors that were used to configure the priors for WHAM (see Supplementary Materials).

With movement as configured, the northern origin fish (ages 2+) can occur in the southern region on January 1. Estimating initial numbers at age as separate parameters can be challenging even in single-stock models, but for black sea bass the available data cannot distinguish the proportion of northern and southern component fish at each age in the southern region in the initial year of the model. Therefore, we used the simplifying equilibrium assumption where there are two parameters estimated for each stock component: an initial recruitment and an equilibrium fully-selected F (across all fleets) that determines the initial abundance at age in each region for each stock component.

For subsequent years, all models allow AR1 correlation of recruitment and 2DAR1 correlation for apparent survival random effects for both the northern and southern stock components. Models with apparent survival random effects will model the transitions (conditional on both survival and movement) of abundances at age of northern origin fish in each region, but there appears to be little ability of the existing data from the southern region to distinguish apparent survival random effects for each stock component. All models we considered assume a very small variance for the transitions of northern fish in the southern region, which is essentially the same as the deterministic transition assumptions of a statistical catch at age model. Unique variance and correlation parameters for the recruitment and apparent survival random effects are estimated for the northern and southern components.

Uncertainty in recreational index observations

The estimated coefficients of variation (CVs) provided by the analyses by the Working Group to generate the recreational catch per angler (recreational CPA) index ranged between 0.02 and 0.06 which the Working Group felt did not capture the true observation uncertainty in the index with regard to its relationship to stock abundance. All models we considered allowed a scalar multiple of the standard deviation of the log aggregate index to be estimated for these indices in the northern and southern regions. Although lack of

model convergence was observed in many fits for self-test simulations, the estimation of critical model output (e.g., SSB, fishing mortality) was reliable and robust to the poor estimation of these scalars (Figure S3), and estimating these parameters rather than fixing them in the fit to the actual data allows uncertainty in model output to be more properly conveyed.

Index and catch age composition observations

The Working Group investigated many alternative assumptions for the probability models and selectivity forms for the eight different sets of age composition observations to reduce residual and retrospective patterns. These analyses resulted in use of selectivity random effects for the northern fleet and indices, logistic-normal likelihoods for six sets of age composition observations, and Dirichlet-multinomial likelihoods for one index and one fleet in the northern region (Table S1).

Bottom temperature effects

All models include observations of winter bottom temperature anomalies for the northern and southern regions from 1959 to 2021 and standard errors of observations ranged between 0.03 and 0.09 degrees Celsius (NEFSC 2023). See the Supplementary Materials for details about the derivation of these observations. We retained the assumption from the peer-reviewed assessment that treated the latent bottom temperature covariates in each region as AR1 processes.

We fit 14 models with alternative assumptions about the effects of bottom temperature covariates, ranging from no effects to effects on both regions for either recruitment or natural mortality at age 1 (Table 1). These analyses derive from the hypothesis that bottom temperature affects survival over the first winter where fish turn from age 0 to age 1 on January 1 (Miller et al. 2016a). This covariate may be a proxy for temperature prior to January 1 and affect survival during the end of the pre-recruit phase or natural mortality in the early part of the year after becoming age 1. Furthermore, we have no direct observations of age 1 individuals from surveys until the spring season each year. Therefore, we fit models with effects of temperature on recruitment or natural mortality at age 1.

All models treat annual recruitment as AR1 time-varying random effects with mean parameters for each stock component. However, Miller et al. (2018) showed how inferences of temperature effects on growth or maturity parameters can be very different depending on whether the compared models with and without the effect also include random effects representing residual temporal variation in parameters. Therefore, we also explored whether including temporal random effects on age 1 natural mortality affected inferences

on corresponding temperature effects. Initially, we included random effects on age 1 natural mortality for both the northern and southern stock components, but estimates of these random effects and corresponding variance for the southern component converged to 0 so these were not included in models presented here.

We assume the covariate in year y affects recruitment in the same year because the covariate observations are from winter months. The fish are technically already 1 year old, but there are no observations of these individuals until later in the spring except possibly in fishery catches which are accumulated over the whole year. Expected log-recruitment for a given stock component is a linear function of bottom temperature

$$E(\log N_{y,1}|x_y) = \mu_R + \beta_R x_y. \quad (11)$$

Similarly, expected log-natural mortality as a function of bottom temperature is

$$E(\log M_{y,1}|x_y) = \mu_{M,1} + \beta_M x_y. \quad (12)$$

Because age 1 fish for the northern component can exist in both regions after January 1 other the spawning period, natural mortality is acting in both regions for this stock. For models with covariate and(or) annual random effects for age 1 fish we assume them only in the northern region for the northern component. The corresponding random effects are

$$\log N_{y,1} = E(\log N_{y,1}|x_y) + \varepsilon_{y,1} \quad (13)$$

and

$$\log M_{y,1} = E(\log M_{y,1}|x_y) + \varepsilon_{M,y}. \quad (14)$$

The constant or mean log-natural mortality rate is assumed to be $\mu_{M,a} = \log(0.4)$ for all ages as recommended by the Working Group. Because the bottom temperature anomalies and random effects are centered at 0, mean log-natural mortality at age 1 over the time series should be approximately equal to $\mu_{M,1}$ for models that include those effects.

Model fitting and diagnostics

We used a development version (commit 53e236b) of the WHAM package after the release of version 2.0 for all results. All code for fitting models and generating results can be found at github.com/timjmiller/multi_wham_bsb.

We examined retrospective patterns for all models by fitting corresponding models where the terminal year

is reduced sequentially by one year (peel) for seven years. Therefore, there are eight fits of each model with the time series reduced by zero to seven years. We calculated Mohn’s ρ for SSB, and average F at ages 6 and 7. Absolute values of Mohn’s ρ near 0 imply no pattern in estimation of these quantities as the time-series is sequentially extended. As in Miller et al. (2016b), we also assessed the consistency of the AIC-based model selection over retrospective peels to guard against previously noted changes in perception of covariate effects on recruitment with increased length of the time series of observations (Myers 1998). This retrospective examination was also recommended by Brooks (2024).

We performed a jitter analysis of the base model M_0 and the best fitting model to investigate whether a local minimum of the negative log-likelihood surface was obtained by the optimization. We used the jitter_wham function in the WHAM package which by default simulates starting values from a multivariate normal distribution with mean and covariance defined by the MLEs and hessian-based covariance matrix from the fitted model. See the Supplementary Materials for more details.

For the best performing model, we also performed simulation self-tests where new observations were simulated conditional on all estimated fixed and random effects and the same model configuration was fit to each of the simulated data sets. We estimated median relative bias of SSB across these simulations. Finally, we fitted three sensitivity models which differed from the best performing model, by 1) assuming no movement for either stock component, 2) movement parameters are fixed at the means for the prior distributions, and 3) a constant natural mortality rate is estimated across all regions and stocks. See the Supplementary Materials for more details.

Reference points and projections

We produced SPR-based BRP estimates ($F_{40\%}$ and $SSB_{40\%}$) from the best performing model using a variety of options provided in WHAM. We generated annual BRP estimates based on the annual weight at age, maturity at age, natural mortality, fleet selectivity, and either the annual recruitment random effect (Eq. 13) or the annual expected recruitment (Eq. 11). We also calculated status as the ratios of annual average F and SSB to the corresponding reference points. Finally, we calculated “prevailing” BRPs using the average weight at age, maturity at age, M , and fleet selectivity from the last 5 years (2017 to 2021) and average recruitment over years 2000 to 2021, and made Kobe plots of joint status for the terminal year of the model (2021). All BRPs and status estimates are generated for each region as well as for the total stock area.

We projected the best black sea bass model under three alternative scenarios for the bottom temperature covariate where 1) the AR1 time-series model continues into the projection years, 2) the average of the most

recent 5 years is projected, and 3) bottom temperature increases in projection years following a prediction from a simple linear regression of the estimated bottom temperature anomalies over time. We specified fishing mortality in projection years to be constant at the value in the last model year (2021). Average weight, natural mortality, movement, and maturity at age over the last 5 years are used in projection years whereas the AR1 processes for all numbers at age random effects are continued.

Results

We found the best model of bottom temperature covariate effects included the effect only on recruitment of the northern stock component and no random effects on age 1 natural mortality (M_1 , Tables 2 and S2). Model M_1 consistently had the lowest AIC across retrospective peels where the terminal years of data are removed from the model. The difference in AIC for the model that also included bottom temperature effects on recruitment for the southern component (M_3) suggested some evidence for this hypothesis as well. There was little evidence for also including random effects on age 1 natural mortality for the northern stock component. However, when more than three terminal years of data were removed, the evidence for adding age 1 natural mortality random effects for the northern component (M_8) increased similar to adding bottom temperature effects on southern component recruitment (M_3).

Comparisons of estimates from retrospective peels did not show any indication of differences in model performance. There was little variation in measures of retrospective patterns for SSB or fishing mortality across models. Mohn's $\rho \approx -0.03$ for SSB of both stock components and Mohn's $\rho \approx 0.03$ and ≈ -0.04 for average F at ages 6 and 7 in north and south regions, respectively (Table 3).

Estimated positive effects of bottom temperature on recruitment for the northern or southern components were stable over the retrospective peels and differed negligibly whether effects for each component were estimated in isolation or together (Table 4). The estimates for the effects on each stock component were essentially equivalent whether the effect was on one component or both. Estimates of residual variability in northern component recruitment, as measured by the conditional or marginal standard deviation of the recruitment random effects, increased slightly with the number of peeled years. However, the ratio of standard deviations of models with and without temperature effects was stable with approximately 20% reduction in residual standard deviation when temperature effects were included. The residual variation is reduced because the expected recruitment (Eq. 11) is a function of the covariate (Figure S5).

The posterior estimates of the bottom temperature covariate match the observations well because of the high precision of the observed anomalies (Figure S4). The anomalies for the north and south regions appear highly

correlated presumably because of the proximity of the two regions. Because the temperature anomalies are treated as latent variables, other data components in the model can affect the estimated anomalies when effects on recruitment are included (e.g., Miller et al. 2018), but in this case the estimates of anomalies are altered negligibly during the population model years when the effect on recruitment is estimated (Figure S7).

The effect of the anomalies on expected recruitment can be better observed by comparing the time series of the northern and southern components (Figure 4). The expected recruitment for the southern component without any covariate effects is constant over time whereas the effect of the anomalies on expected recruitment for the northern component induces annual variation in expected recruitment. The annual variation in expected recruitment (and the temperature anomalies) is correlated with the recruitment random effects of the northern component and therefore reduces the residual variation in the recruitment random effects. For the northern stock component, most of the lowest estimated recruitment random effects occurred prior to 2000 and several large recruitment estimates occurred after 2010. For the southern stock component, recruitment random effect estimates have been less variable and similar to the estimated median particularly since 2005. The estimated size of the northern stock component, as measured by SSB, increased substantially since 2005, whereas that for the southern component peaked in 2002. The increase in the northern component is also reflected in the total size of the combined components. Estimated average total fishing mortality rates across ages 6 and 7 (combining the commercial and recreational fleets) were highest in the southern region prior to 1998 and have declined substantially since then. Estimated fishing mortality rates in the northern region have been less variable, but had largest peaks in 1996, 1999, and 2005. The decline in estimates in the southern component is also reflected in the decline in total fishing mortality across regions.

The estimated movement from the north to the south for the northern stock component is much less than anticipated from the prior distribution that was parameterized based on the companion Stock Synthesis model fit completed by the Working Group (Figure 3). Conversely, the estimated movement rate from south to north was more consistent and slightly greater than that from the companion model. The estimated movement rates varied little across all fitted models implying that the estimation of movement was not sensitive to the alternative assumptions we considered. Furthermore, the very low estimated movement rate from north to south is also consistent with preliminary fits of the WHAM model without the prior distribution where the movement rate was estimated at the lower bound of 0 resulting in a lack of convergence. The estimated movement rates imply that a very small fraction of northern fish are ever in the southern region.

The 2DAR1 random effects for the selectivity parameters of the northern recreational fleet indicate a decrease in selectivity at ages 2 to 6 over the time series which corresponds to increases in the size limits in regulations

by states where these catches occurred (Figure 5). The model also estimated a more modest decrease in selectivity at ages 2 to 3 for the northern commercial fleet. The selectivity at the youngest ages for the two fishery independent indices varied over time but without notable trend. The selectivity of fleets and indices in the south increased with age, but were constant over time (Figure S8).

The three sensitivity fits suggest the estimates of stock size and fishing mortality are fairly robust to whether the movement rates are fixed at the values from the companion Stock Synthesis fit or whether no movement is assumed (Figure S16). A constant natural mortality rate was estimable, but the estimated rate (0.72) is nearly twice that determined by the Working Group and resulted in generally higher stock sizes and lower fishing mortality rates.

Reference points

Using the expected recruitment rather than the random effects as the multiplier with equilibrium spawning biomass per recruit ($\phi(\tilde{F})$, eq. 7) results in less variable estimates of annual $SSB_{40\%}$ (Figure 6: top row). Estimates were less variable for the southern stock component than the northern stock component mainly because the expected recruitment is constant for the former whereas that for the northern component varies via the effect of the bottom temperature anomalies. Temporal variation for the southern stock component is mainly caused by annual variation in the inputs to the $\phi(\tilde{F})$ calculation and $F_{40\%}$, but there is also some effect of the variation in the proportion of total recruitment for each stock component as used in the weighting terms to define the 40% reduction in unfished spawning biomass per recruit (λ_s in Eq. 10). Using the recruitment random effects instead of expected recruitment creates more uncertain estimates of $SSB_{40\%}$ for the southern stock component whereas there is little difference for the northern component because there is less difference in the types of recruitment estimates resulting from the covariate effects (Figure S11).

Ratios of SSB to $SSB_{40\%}$ should be viewed with caution because the SSB reference point is being defined using annual recruitments rather than some form of average recruitment and therefore, ratios larger than 2.5 which would correspond to unfished population sizes are possible (Figure 6: second row). However, for the southern component, using the constant expected recruitment is comparable to using median recruitment and the annual variation in the inputs to $\phi(\tilde{F})$ indicates no years where SSB was greater than unfished levels throughout the time series. The patterns in uncertainty of SSB ratios are the same as those for the SSB reference points (Figure S15).

Differences between annual $F_{40\%}$ estimates using the alternative types of recruitment estimates are much less than those for $SSB_{40\%}$ because the recruitment estimates are only used in the weighting of the stock

component-specific $\phi(\tilde{F})$ to determine $F_{40\%}$ (λ_s in Eq. 10, Figure 6: third row). For similar reasons, estimates of uncertainty of $F_{40\%}$ are also similar between the type of recruitment estimates (Figure S10). Annual estimates for the northern stock component were lowest in the earliest years of the time series whereas those for the southern component are relatively stable over time.

For a given type of recruitment used to calculate $F_{40\%}$, the annual ratios of average F to the corresponding reference point are identical for each stock component and in total because of the selectivity used to define a single F reference point across both regions is exactly the same as that for the annual estimate of fishing mortality at age by fleet (Figure 6: fourth row). As for annual $F_{40\%}$, estimates of uncertainty in the ratios are similar whether expected recruitment or the random effects are used to calculate the reference points (Figure S14).

Unlike the annual ratios of F to $F_{40\%}$, the $F_{40\%}$ under prevailing conditions uses a selectivity defined by the average F at age and fleet over the last 5 years, which is different from that of the selectivity in the terminal year and therefore those ratios for each region and in total are different (Figure 6: bottom row). Although the alternative types of recruitment estimates result in different points on the Kobe plots for joint status, the uncertainty in the estimates suggest similar probabilities of alternative quadrants. However, the usage of the confidence regions of the ratios to define probabilities is an approximation because these ratios are functions of both empirical Bayes estimates of random effects as well as maximum likelihood estimates of fixed effects.

Projections

When continuing the AR1 model for the bottom temperature anomalies in the projection years, the uncertainty grows and asymptotes to a level determined by the marginal variance of the process and the predicted value approaches the estimated marginal mean value of approximately 0 (Figure 7). There is no uncertainty in the projected linear trend because the values were specified as known whereas there is a small level of uncertainty in the projections of the recent average based on the uncertainty in the estimated mean. Comparing projected recruitment for the northern and southern stock components, the projected expected recruitment has much lower uncertainty than the projected random effects regardless of whether bottom temperature affects recruitment. For the northern component, CVs of projected expected recruitments are smaller than those of recruitment random effects, but there are larger differences between CVs of projected expected recruitment assuming AR1 and the other scenarios for the future bottom temperature anomalies are made (Figure S9).

Because projected fishing mortality is specified to be the same as that in the terminal year the same uncertainty is also propagated in the projections (Figure 8). As we would expect, there is no effect of alternative assumptions about bottom temperature in the projections for the southern stock component because the effect of the bottom temperature anomaly is only on the northern component. However, the alternative bottom temperature assumptions do affect projections of northern component SSB and the projections do not stabilize when the anomalies are projected to increase linearly. When the same AR1 assumption for the bottom temperature anomalies is used in projections, CVs of northern and total SSB projections are larger than when the recent average or linear trend are assumed (Figure S9).

Unlike the annual reference points during the model years (prior to 2022), components of the $\phi(\tilde{F})$ calculations are constant in the projection years where the only changing annual values are the recruitments used in the weighting for $F_{40\%}$ and the recruitments used to calculate the resulting $SSB_{40\%}$ (Figure 9). Estimated reference points in the first few projection years can differ depending on whether the expected recruitment or the random effects are used in their calculation, but longer term projected values are identical because the random effect estimates approach the expected values as the influence of observations diminishes. However, the estimates of uncertainty in the longer term reference points is lower using the expected recruitment rather than the random effects (Figures S10 and S11). The reduction in uncertainty using expected recruitment is less for $F_{40\%}$ than $SSB_{40\%}$ and for the northern component which includes bottom temperature effects than the southern component.

Discussion

Black sea bass

In our investigation of bottom temperature effects on recruitment and natural mortality and time-varying random effects on natural mortality at age 1, we found only including effects on recruitment for the northern stock component to be the best model with respect to AIC. Black sea bass in the NEUS is at the northern extent of its range and the estimated increase in expected recruitment with temperature for the northern stock component is consistent with its range extension to the north (McMahan et al. 2020). Opposite effects of temperature on recruitment or population size would be expected for species in the same general area that are at the southern extent of their range (Gabriel 1992). For example, higher recruitment of the Southern New England-Mid-Atlantic stock of yellowtail flounder is correlated with more cold water persistence into summer and fall on the Northeast US shelf (Sullivan et al. 2005; Miller et al. 2016b).

Our finding regarding bottom temperature effects is consistent with the bottom temperature effects on recruitment in the assessment model accepted during the peer-review process and which is currently used to assess the stock (NEFSC 2023). However, AIC suggested some weight for models with temperature effects on recruitment for the southern component and random effects on M at age 1. Although this might suggest making inferences on the population by using an ensemble of these and weighting by AIC (Burnham and Anderson 2002), the estimates of assessment outputs relevant for management (e.g., SSB and F) were similar among the models and weighted estimates would differ very little from the estimates with the lowest AIC. Continued monitoring of temperature effects on the southern component and investigations of non-linear effects of temperature for both components may be prudent because of the possibility of an optimal temperature range for survival via effects on growth during the pre-recruit phase (Ware and Lambert 1985; Anderson 1988). Furthermore, our inferences about effects on natural mortality at age 1 may be influenced by our assumptions of constant median (or constant depending on the model) natural mortality rate and movement rates for all ages. Further investigations of variation in these parameters with age and effects of bottom temperature could improve our understanding of the demography for this stock.

We showed that using expected recruitment rather than recruitment random effects to define BRPs can produce the same estimates but with lower uncertainty. Although the option is unavailable currently in WHAM, we expect using expected bottom temperature anomalies rather than the random effects would also result in the same BRPs and even lower uncertainty. These results can be important for management when uncertainty in assessment output is used in making catch advice. The typical approach for defining stock and harvest status is to compare BRPs defined under prevailing conditions with current stock and harvest levels, but we could also make the comparisons with projected BRPs like those we demonstrated are possible. The uncertainty in these ratios could also be used in defining catch advice.

BRPs under prevailing conditions use average values for recruitment and other inputs and MSY-based BRPs are based on the stock-recruit relationship which is also typically constant over time. If BRPs should be defined in such a way that they are less variable than the stock over time, expected inputs to the BRPs (instead of annual values) would be more appropriate. Lower variability in BRPs would presumably correlate with lower variability in catch advice which might be desirable (e.g., Cochrane et al. 1998; Kell et al. 2005), but the appropriate level of temporal variability in BRPs and catch advice will depend on the characteristics of the fish stock, associated fisheries, and management structure (Holland 2010; Punt et al. 2016).

For black sea bass, it is evident that the projection methodology of the environmental covariate has an impact on short-term projection estimates of recruitment and SSB (Figures 7 and 8). In the projection period, the

AR1 models for bottom temperature and recruitment revert to the long-term means of those processes. This is most likely not an appropriate assumption for stocks in the NEUS given observations and hypotheses of increasing water temperature and changing environmental conditions (Hare et al. 2016; Pershing et al. 2021). Because of these concerns, the most recent stock assessment for yellowtail flounder used a change point analysis on environmental covariates to determine current conditions. The mean environmental covariate from the current condition was then used as a data input in WHAM to inform short-term projections (NEFSC 2024b). Unfortunately, this methodology still has limitations because it is unlikely that current environmental conditions are stable. Similarly, a linear increase of temperature is also not likely in the future (top row of Figure 4). As more assessments begin including effects of environmental covariates explicitly in assessment models, assumptions about these covariates in BRPs and population projections becomes an important decision in the management process.

General model

WHAM provides a large class of models for time- and age-varying random effects for population attributes and treatment of environmental covariates and their effects on populations using state-space methods (Maunder 2024). This framework accounts for the magnitude of differing uncertainties in observations and stochastic population dynamics processes. Version 2.0 extends these inferences to movement rates for multi-region models and stock (component) specific configuration of random and environmental covariate effects.

An obvious limitation to WHAM is the inability to include tagging observations of any type. Such observations are critical to estimation of movement parameters (e.g., Goethel et al. 2019). We used estimates of movement parameters from a companion assessment model to define prior distributions for corresponding movement parameters in the state-space black sea bass model, but other than the tagging data, both of the assessment models used much the same data which can lead to inappropriate inferences. In lieu of integrating an observation model for the tagging data, a better approach would be to estimate the movement parameters externally from just the tagging data.

Tagging data can also inform mortality rate parameters (Hampton 1991). It is well known that natural mortality is seldom estimated in assessment models because the observed data often provide little information to distinguish natural mortality from other assessment model parameters (Lee et al. 2011; Clark 2022). Estimation of natural mortality may be even more challenging within state-space assessment models with their greater flexibility from inclusion of time-varying random effects. For example, we fixed the mean natural mortality for age 1 fish and both Cadigan (2016) and Stock et al. (2021) also estimated natural mortality

deviations. However, the simulation studies of Miller et al. (In review) suggest estimating natural mortality in WHAM is feasible in some situations with typical assessment data. Regardless, tagging observations can provide improved inferences and allowing tagging observations in WHAM should be a high priority even for models with a single stock and region. This extension would also be beneficial for black sea bass because the current assessment uses much the same data to estimate movement outside of the model as we are using to estimate the other parameters in the WHAM model.

WHAM version 2.0 only allows models where each stock spawns and recruits in a single region however, some stocks are assessed with spatial units that are assumed to have a global stock and recruitment model that distributes recruitment to each region (Kapur et al. 2021). Therefore, extending WHAM to allow such models would be beneficial. Finally, because age composition data are scarce for many stocks, incorporating the work by Correa et al. (2023) on allowing length composition and modeling growth within WHAM would provide an assessment tool to include process errors in assessment with such data and possibly with multiple stocks and regions.

Our application to black sea bass is a particular combination of the spatial modeling options described by Berger et al. (2024). Other combinations of the described options are possible in WHAM 2.0. For example, WHAM 2.0 can accommodate all of fleet structure options described in Table 2 by Berger et al. (2024) and we expect more of these options to become available in future versions of WHAM.

Acknowledgements

We express our gratitude to the many scientists who have collected and processed the data that went into the assessment model, including survey biologists, port samplers, observers and agers. We thank the black sea bass research track assessment working group and peer-reviewers for the work compiling data and determining many of the configurations of the black sea bass assessment model that we used for our analyses. We also thank Chris Legault, two anonymous reviewers, and the associate editor for comments and suggestions that improved the clarity of this paper.

References

- Able, K.W., and Stanton Hales, Jr., L. 1997. Movements of juvenile black sea bass *Centropristis striata* (linnaeus) in a southern New Jersey estuary. *Journal of Experimental Marine Biology and Ecology* **213**(2): 153–167. doi:10.1016/S0022-0981(96)02743-8.

- Andersen, P.K., and Keiding, N. 2002. Multi-state models for event history analysis. *Statistical Methods in Medical Research* **11**: 91–115. doi:10.1191/0962280202SM276ra.
- Anderson, J.T. 1988. A review of size dependent survival during pre-recruit stages of fishes in relation to recruitment. *Journal of Northwest Atlantic Fishery Science* **8**: 55–66. doi:10.2960/J.v8.a6.
- Arnason, A.N. 1972. Parameter estimates from mark-recapture experiments on two populations subject to migration and death. *Researches on Population Ecology* **13**: 97–113. doi:10.1007/BF02521971.
- ASMFC. 2016. Black sea bass stock assessment. Available at <http://www.asmf.org/uploads/file/5953f11d2016BlackSeaBassS>
- Bell, R.J., Richardson, D.E., Hare, J.A., Lynch, P.D., and Fratantoni, P.S. 2015. Disentangling the effects of climate, abundance, and size on the distribution of marine fish: An example based on four stocks from the Northeast US shelf. *ICES Journal of Marine Science* **72**(5): 1311–1322. doi:10.1093/icesjms/fsu217.
- Berger, A.M., Barceló, C., Goethel, D.R., Hoyle, S.D., Lynch, P.D., McKenzie, J., Dunn, A., Punt, A.E., Methot, R.D., Hampton, J., Porch, C.E., McGarvey, R., Thorson, J.T., A’mar, Z.T., Deroba, J.J., Elvarsson, B.P., Holmes, S.J., Howell, D., Langseth, B.J., Marsh, C., Maunder, M.N., Mormede, S., and Rasmussen, S. 2024. Synthesizing the spatial functionality of contemporary stock assessment software to identify future needs for next generation assessment platforms. *Fisheries Research* **275**: 107008. doi:10.1016/j.fishres.2024.107008.
- Bosley, K.M., Schueller, A.M., Goethel, D.R., Hanselman, D.H., Fenske, K.H., Berger, A.M., Deroba, J.J., and Langseth, B.J. 2022. Finding the perfect mismatch: Evaluating misspecification of population structure within spatially explicit integrated population models. *Fish and Fisheries* **23**(2): 294–315. doi:10.1111/faf.12616.
- Brooks, E.N. 2024. Pragmatic approaches to modeling recruitment in fisheries stock assessment: A perspective. *Fisheries Research* **270**: 106896. doi:10.1016/j.fishres.2023.106896.
- Burnham, K.P., and Anderson, D.R. 2002. Model selection and multimodel inference: A practical information-theoretic approach. Springer-Verlag, New York.
- Cadigan, N.G. 2016. A state-space stock assessment model for northern cod, including under-reported catches and variable natural mortality rates. *Canadian Journal of Fisheries and Aquatic Sciences* **73**(2): 296–308. doi:10.1139/cjfas-2015-0047.
- Cao, J., Truesdell, S.B., and Chen, Y. 2014. Impacts of seasonal stock mixing on the assessment of Atlantic cod in the Gulf of Maine. *ICES Journal of Marine Science* **71**(6): 1443–1457. doi:10.1093/icesjms/fsu066.
- Clark, W.G. 2022. Why natural mortality is estimable, in theory if not in practice, in a data-rich stock assessment. *Fisheries Research* **248**: 106203. doi:10.1016/j.fishres.2021.106203.
- Cochrane, K.L., Butterworth, D.S., De Oliveira, J.A.A., and Roel, B.A. 1998. Management procedures in a fishery based on highly variable stocks and with conflicting objectives: Experiences in the South African

- pelagic fishery. *Reviews in Fish Biology and Fisheries* **8**(2): 177–214. doi:10.1023/A:1008894011847.
- Commenges, D. 1999. Multi-state models in epidemiology. *Lifetime Data Analysis* **5**: 315–327. doi:10.1023/A:1009636125294.
- Correa, G.M., Monnahan, C.C., Sullivan, J.Y., Thorson, J.T., and Punt, A.E. 2023. Modelling time-varying growth in state-space stock assessments. *ICES Journal of Marine Science* **80**(7): 2036–2049. doi:10.1093/icesjms/fsad133.
- du Pontavice, H., Chen, Z., and Saba, V.S. 2023. A high-resolution ocean bottom temperature product for the northeast U.S. Continental shelf marine ecosystem. *Progress in Oceanography* **210**: 102948. doi:10.1016/j.pocean.2022.102948.
- Fabrizio, M.C., Manderson, J.P., and Pessutti, J.P. 2013. Habitat associations and dispersal of black sea bass from a Mid-Atlantic Bight reef. *Marine Ecology Progress Series* **482**: 241–253. doi:10.3354/meps10302.
- Francis, R.I.C.C. 2014. Replacing the multinomial in stock assessment models: A first step. *Fisheries Research* **151**: 70–84. doi:10.1016/j.fishres.2013.12.015.
- Gabriel, W.L. 1992. Persistence of demersal fish assemblages between Cape Hatteras and Nova Scotia, Northwest Atlantic. *Journal of the Northwest Atlantic Fisheries Science* **14**(1): 29–46.
- Goethel, D.R., Bosley, K.M., Hanselman, D.H., Berger, A.M., Deroba, J.J., Langseth, B.J., and Schueller, A.M. 2019. Exploring the utility of different tag-recovery experimental designs for use in spatially explicit, tag-integrated stock assessment models. *Fisheries Research* **219**: 105320. doi:10.1016/j.fishres.2019.105320.
- Hampton, J. 1991. Estimation of southern bluefin tuna *Thunnus maccoyii* natural mortality and movement rates from tagging experiments. *Fishery Bulletin* **89**(4): 591–610.
- Hare, J.A., Morrison, W.E., Nelson, M.W., Stachura, M.M., Teeters, E.J., Griffis, R.B., Alexander, M.A., Scott, J.D., Alade, L., Bell, R.J., Chute, A.S., Curti, K.L., Curtis, T.H., Kircheis, D., Kocik, J.F., Lucey, S.M., McCandless, C.T., Milke, L.M., Richardson, D.E., Robillard, E., Walsh, H.J., McManus, M.C., Marancik, K.E., and Griswold, C.A. 2016. A vulnerability assessment of fish and invertebrates to climate change on the northeast U.S. Continental shelf. *PLOS ONE* **11**: 1–30. doi:10.1371/journal.pone.0146756.
- Hearn, W.S., Sundland, R.L., and Hampton, J. 1987. Robust estimation of the natural mortality rate in a completed tagging experiment with variable fishing intensity. *Journal Du Conseil International Pour L’exploration De La Mer* **43**: 107–117. doi:10.1093/icesjms/43.2.107.
- Holland, D. 2010. Management strategy evaluation and management procedures: Tools for rebuilding and sustaining fisheries. OECD Publishing, Paris. doi:10.1787/5kmd77jhvkjf-en.
- Kapur, M.S., Siple, M.C., Olmos, M., Privitera-Johnson, K.M., Adams, G., Best, J., Castillo-Jordán, C., Cronin-Fine, L., Havron, A.M., Lee, Q., Methot, R.D., and Punt, A.E. 2021. Equilibrium reference

- point calculations for the next generation of spatial assessments. *Fisheries Research* **244**: 106132. doi:10.1016/j.fishres.2021.106132.
- Kell, L.T., Pastoors, M.A., Scott, R.D., Smith, M.T., Van Beek, F.A., O'Brien, C.M., and Pilling, G.M. 2005. Evaluation of multiple management objectives for northeast Atlantic flatfish stocks: Sustainability vs. Stability of yield. *ICES Journal of Marine Science* **62**(6): 1104–1117. doi:10.1016/j.icesjms.2005.05.005.
- Kemeny, J.G., and Snell, J.L. 1960. *Finite Markov chains*. D. Van Nostrand Company, Princeton, New Jersey.
- Kristensen, K., Nielsen, A., Berg, C., Skaug, H., and Bell, B.M. 2016. TMB: Automatic differentiation and Laplace approximation. *Journal of Statistical Software* **70**: 1–21. doi:10.18637/jss.v070.i05.
- Lee, H.-H., Maunder, M.N., Piner, K.R., and Methot, R.D. 2011. Estimating natural mortality within a fisheries stock assessment model: An evaluation using simulation analysis based on twelve stock assessments. *Fisheries Research* **109**(1): 89–94. doi:10.1016/j.fishres.2011.01.021.
- Legault, C.M., and Restrepo, V.R. 1999. A flexible forward age-structured assessment program. *Col. Vol. Sci. Pap. ICCAT* **49**(2): 246–253.
- Maunder, M.N. 2024. Towards a comprehensive framework for providing management advice from statistical inference using population dynamics models. *Ecological Modelling* **498**: 110836. doi:10.1016/j.ecolmodel.2024.110836.
- McMahan, M.D., Sherwood, G.D., and Grabowski, J.H. 2020. Geographic variation in life-history traits of black sea bass (*Centropristis striata*) during a rapid range expansion. *Frontiers in Marine Science* **7**: 567758. doi:10.3389/fmars.2020.567758.
- Methot, R.D., and Wetzel, C.R. 2013. Stock Synthesis: A biological and statistical framework for fish stock assessment and fishery management. *Fisheries Research* **142**(1): 86–99. doi:10.1016/j.fishres.2012.10.012.
- Miller, A.S., Shepherd, G.R., and Fratantoni, P.S. 2016a. Offshore habitat preference of overwintering juvenile and adult black sea bass, *Centropristis striata*, and the relationship to year-class success. *PLOS ONE* **11**(1): e0147627. doi:10.1371/journal.pone.0147627.
- Miller, T.J., and Andersen, P.K. 2008. A finite-state continuous-time approach for inferring regional migration and mortality rates from archival tagging and conventional tag-recovery experiments. *Biometrics* **64**(4): 1196–1206. doi:10.1111/j.1541-0420.2008.00996.x.
- Miller, T.J., Britten, G., Brooks, E.N., Fay, G., Hansell, A., Legault, C.M., Li, C., Muffley, B., Stock, B.C., and Wiedenmann, J. In review. An investigation of factors affecting inferences from and reliability of state-space age-structured assessment models. *Canadian Journal of Fisheries Science*.
- Miller, T.J., Hare, J.A., and Alade, L.A. 2016b. A state-space approach to incorporating environmental effects on recruitment in an age-structured assessment model with an application to southern New

- England yellowtail flounder. Canadian Journal of Fisheries Science **73**(8): 1261–1270. doi:10.1139/cjfas-2015-0339.
- Miller, T.J., O'Brien, L., and Fratantoni, P.S. 2018. Temporal and environmental variation in growth and maturity and effects on management reference points of Georges Bank Atlantic cod. Canadian Journal of Fisheries Science **75**(12): 2159–2171. doi:10.1139/cjfas-2017-0124.
- Miller, T.J., and Stock, B.C. 2020. The Woods Hole Assessment Model (WHAM). <https://timjmiller.github.io/wham>.
- Mohn, R. 1999. The retrospective problem in sequential population analysis: An investigation using cod fishery and simulated data. ICES Journal of Marine Science **56**(4): 473–488. doi:10.1006/jmsc.1999.0481.
- Moser, J., and Shepherd, G.R. 2009. Seasonal distribution and movement of black sea bass (*Centropristis striata*) in the Northwest Atlantic as determined from a mark-recapture experiment. Journal of Northwest Atlantic Fishery Science **40**: 17–28.
- Musick, J.A., and Mercer, L.P. 1977. Seasonal distribution of black sea bass, *Centropristis striata*, in the Mid-Atlantic Bight with comments on the ecology and fisheries of the species. Transactions of the American Fisheries Society **106**(1): 12–25. doi:10.1577/1548-8659(1977)106<12:SDOBSB>2.0.CO;2.
- Myers, R.A. 1998. When do environment–recruitment correlations work? Reviews in Fish Biology and Fisheries **8**(3): 229–249. doi:10.1023/A:1008828730759.
- NEFSC. 2022a. Final report of the haddock research track assessment working group. Available at https://s3.us-east-1.amazonaws.com/nefmc.org/14b_EGB_Research_Track_Haddock_WG_Report_DRAFT.pdf.
- NEFSC. 2022b. Report of the american plaice research track working group. Available at https://s3.us-east-1.amazonaws.com/nefmc.org/2_American-Plaice-WG-Report.pdf.
- NEFSC. 2023. Report of the black sea bass (*Centropristis striata*) research track stock assessment working group. Available at https://www.mafmc.org/s/a_2023_BSB_UNIT_RTWG_Report_V2_12_2_2023-1.pdf.
- NEFSC. 2024a. Butterfish research track assessment report. US Dept Commer Northeast Fish Sci Cent Ref Doc. 24-03; 191 p.
- NEFSC. 2024b. The yellowtail flounder research track assessment report. Available at <https://www.fisheries.noaa.gov/inport/>. Accessed on 1/10/2025.
- Nielsen, A., and Berg, C.W. 2014. Estimation of time-varying selectivity in stock assessments using state-space models. Fisheries Research **158**: 96–101. doi:10.1016/j.fishres.2014.01.014.
- Perreault, A.M.J., Wheeland, L.J., Morgan, M.J., and Cadigan, N.G. 2020. A state-space stock assessment model for American plaice on the Grand Bank of Newfoundland. Journal of Northwest Atlantic Fishery Science **51**: 45–104. doi:10.2960/j.v51.m727.
- Pershing, A.J., Alexander, M.A., Brady, D.C., Brickman, D., Curchitser, E.N., Diamond, A.W., McCle-

- nachan, L., Mills, K.E., Nichols, O.C., Pendleton, D.E., Record, N.R., Scott, J.D., Staudinger, M.D., and Wang, Y. 2021. Climate impacts on the Gulf of Maine ecosystem: A review of observed and expected changes in 2050 from rising temperatures. *Elementa: Science of the Anthropocene* **9**(1): 00076. doi:10.1525/elementa.2020.00076.
- Punt, A.E., Butterworth, D.S., Moor, C.L. de, De Oliveira, J.A.A., and Haddon, M. 2016. Management strategy evaluation: Best practices. *Fish and Fisheries* **17**(2): 303–334. doi:10.1111/faf.12104.
- Punt, A.E., Dunn, A., Elvarsson, B., Hampton, J., Hoyle, S.D., Maunder, M.N., Methot, R.D., and Nielsen, A. 2020. Essential features of the next-generation integrated fisheries stock assessment package: A perspective. *Fisheries Research* **229**: 105617. doi:10.1016/j.fishres.2020.105617.
- Schwarz, C.J., Schweigert, J.F., and Arnason, A.N. 1993. Estimating migration rates using tag-recovery data. *Biometrics* **49**: 177–193. doi:10.2307/2532612.
- Stock, B.C., and Miller, T.J. 2021. The Woods Hole Assessment Model (WHAM): A general state-space assessment framework that incorporates time- and age-varying processes via random effects and links to environmental covariates. *Fisheries Research* **240**: 105967. doi:10.1016/j.fishres.2021.105967.
- Stock, B.C., Xu, H., Miller, T.J., Thorson, J.T., and Nye, J.A. 2021. Implementing two-dimensional autocorrelation in either survival or natural mortality improves a state-space assessment model for Southern New England-Mid Atlantic yellowtail flounder. *Fisheries Research* **237**: 105873. doi:10.1016/j.fishres.2021.105873.
- Sullivan, M.C., Cowen, R.K., and Steves, B.P. 2005. Evidence for atmosphere–ocean forcing of yellowtail flounder (*Limanda ferruginea*) recruitment in the Middle Atlantic Bight. *Fisheries Oceanography* **14**(5): 386–399. doi:10.1111/j.1365-2419.2005.00343.x.
- Thorson, J.T., Johnson, K.F., Methot, R.D., and Taylor, I.G. 2017. Model-based estimates of effective sample size in stock assessment models using the Dirichlet-multinomial distribution. *Fisheries Research* **192**: 84–93. doi:10.1016/j.fishres.2016.06.005.
- Thorson, J.T., Miller, T.J., and Stock, B.C. 2023. The multivariate-Tweedie: A self-weighting likelihood for age and length composition data arising from hierarchical sampling designs. *ICES Journal of Marine Science* **80**(10): 2630–2641. doi:10.1093/icesjms/fsac159.
- Varkey, D.A., Babyn, J., Regular, P., Ings, D.W., Kumar, R., Rogers, B., Champagnat, J., and Morgan, M.J. 2022. A state-space model for stock assessment of cod (*Gadus morhua*) stock in NAFO subdivision 3Ps. *DFO Can. Sci. Advis. Sec. Res. Doc.* 2022/022. v + 78 p.
- Ware, D.M., and Lambert, T.C. 1985. Early life history of Atlantic mackerel (*Scomber scombrus*) in the southern Gulf of St. Lawrence. *Canadian Journal of Fisheries and Aquatic Sciences* **42**(3): 577–592. doi:10.1139/f85-075.

843 Ying, Y., Chen, Y., Lin, L., and Gao, T. 2011. Risks of ignoring fish population spatial structure in fisheries
844 management. *Canadian Journal of Fisheries and Aquatic Sciences* **68**(12): 2101–2120. doi:10.1139/f2011-
845 116.

Figures

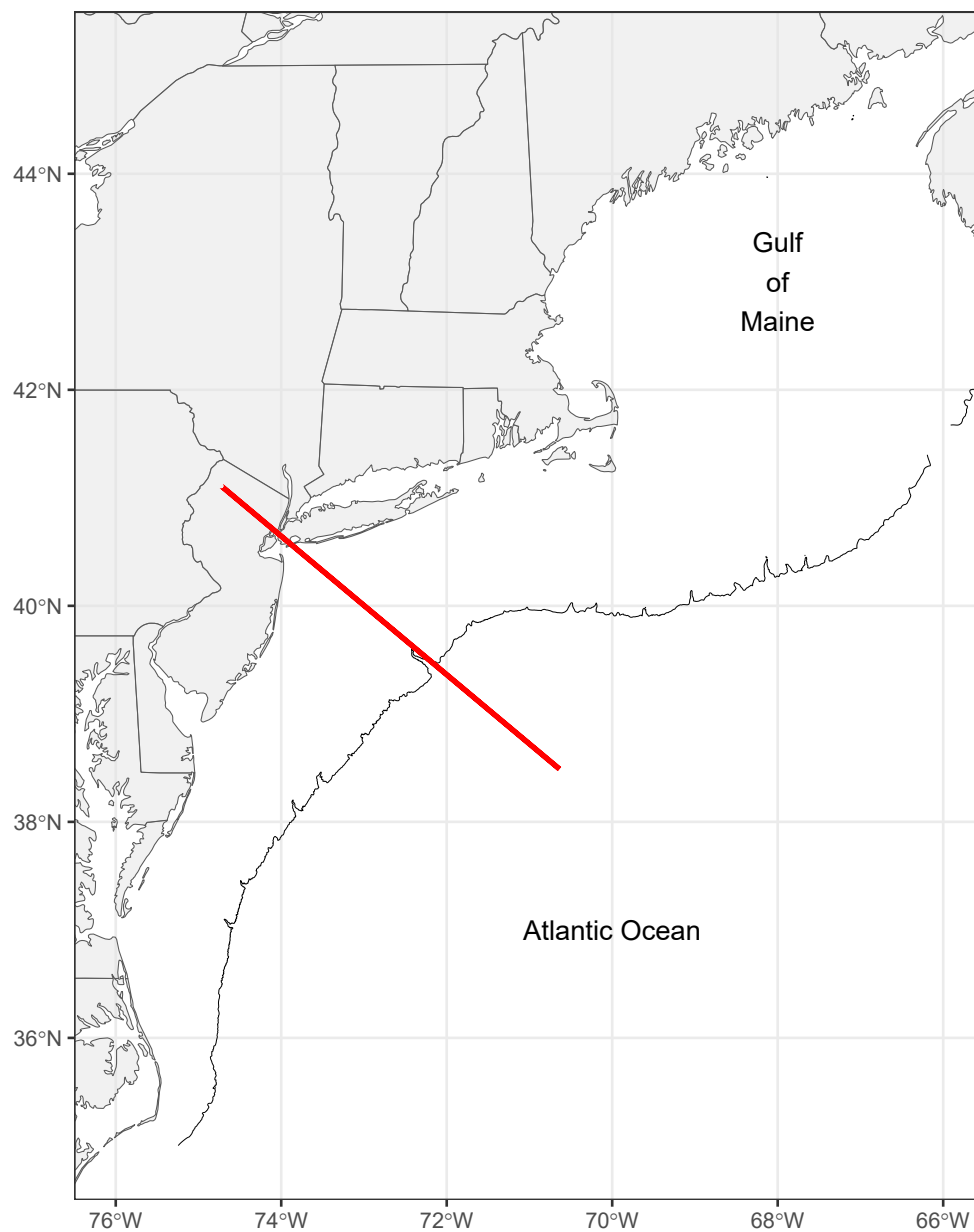


Figure 1: The Northwest Atlantic coastal area where the NEUS black sea bass stock occurs. Red line indicates the Hudson Canyon delineation of northern and southern regions and spawning populations (after Miller et al. 2016a) and the bathymetric contour is the 400 m isocline.

	Jan	Feb	Mar	Apr	May	Jun	Jul	Aug	Sep	Oct	Nov	Dec
Northern Component	Monthly survival and movement north					Survival and spawning		Monthly survival and movement south				
Southern Component	Monthly survival					Survival and spawning		Monthly survival				

Figure 2: Diagram of intervals within the year and configuration of the dynamics of each component of the BSB population.

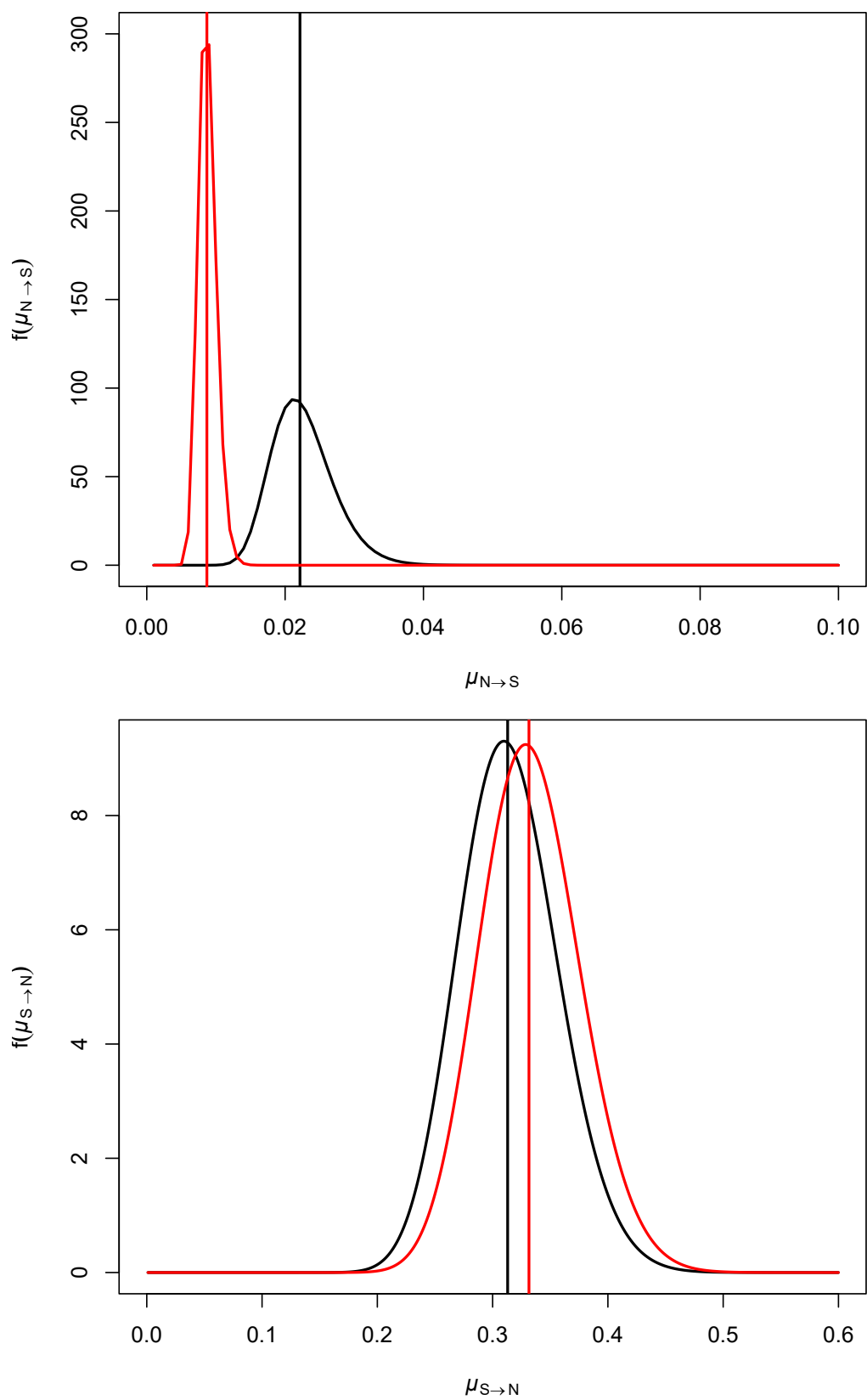


Figure 3: Prior (black) and posterior (red) distributions of movement of the northern stock component from north to south (top) and south to north (bottom). Vertical lines are the prior and posterior estimates.

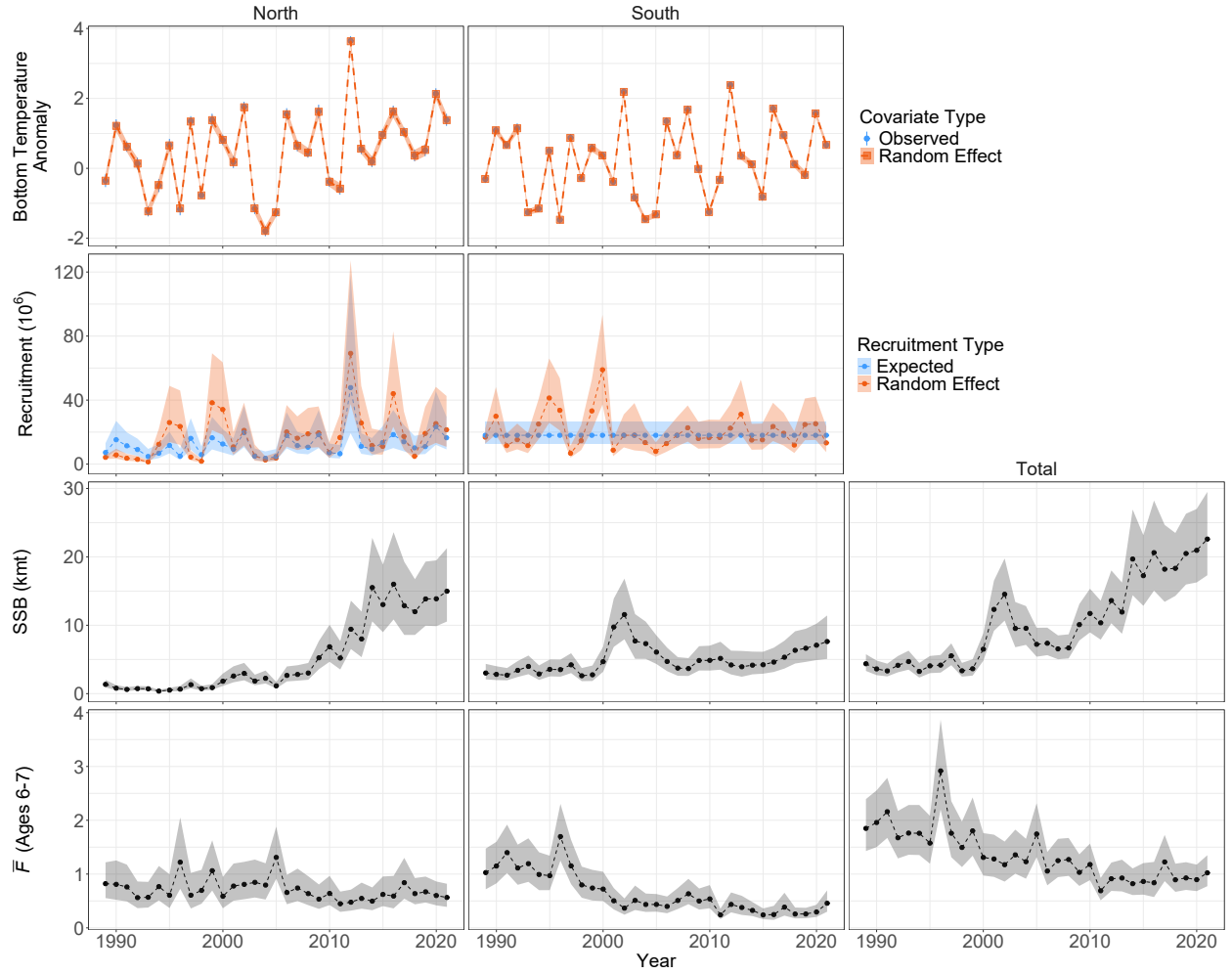


Figure 4: Annual observations and posterior estimates of bottom temperature anomalies (top row), annual expected and random effect recruitment estimates (second row) and SSB and average fishing mortality at ages 6 and 7 from model M_1 . Columns define estimates regionally (spawning region for SSB) and total SSB and fishing mortality across regions. Polygons and vertical lines represent 95% confidence intervals.

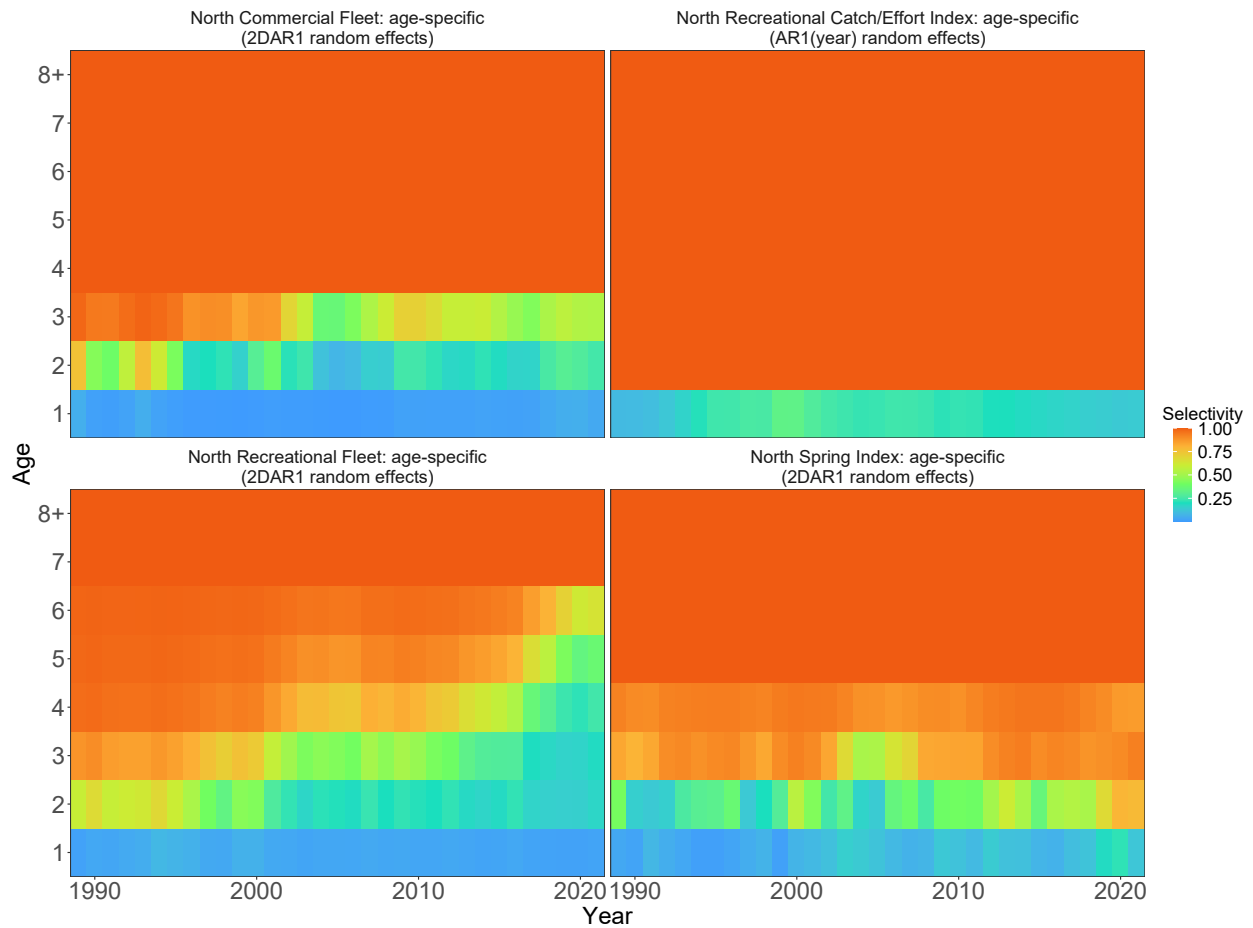


Figure 5: Time and age-varying selectivity for fleets and indices in the northern region with autoregressive random effects.

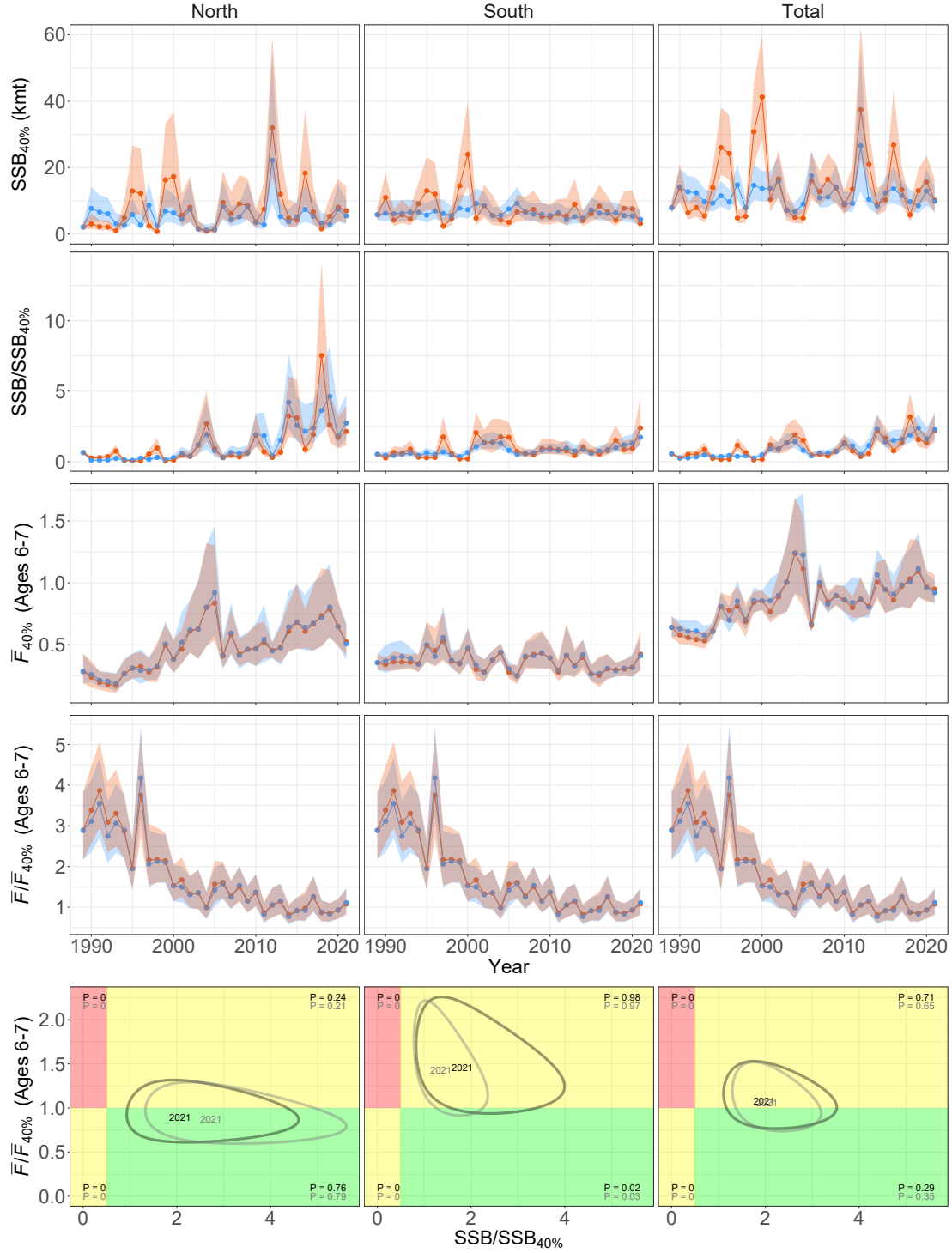


Figure 6: Estimates of average equilibrium F at ages 6 and 7 that produces the 40% spawning potential ratio, equilibrium SSB at $F_{40\%}$ based on annual inputs to $\phi(\tilde{F})$ calculations, annual fishing and biomass status (ratios), and bivariate kobe plots of status in 2021 where reference points represent prevailing conditions with inputs to $\phi(\tilde{F})$ averaged over the last 5 years and recruitment is averaged over the time series. Red and blue in first 4 rows and black and gray in final row indicate alternative annual estimates of recruitment (random effect or expected). All results are based on model M_1 . Polygons represent 95% confidence intervals or regions.

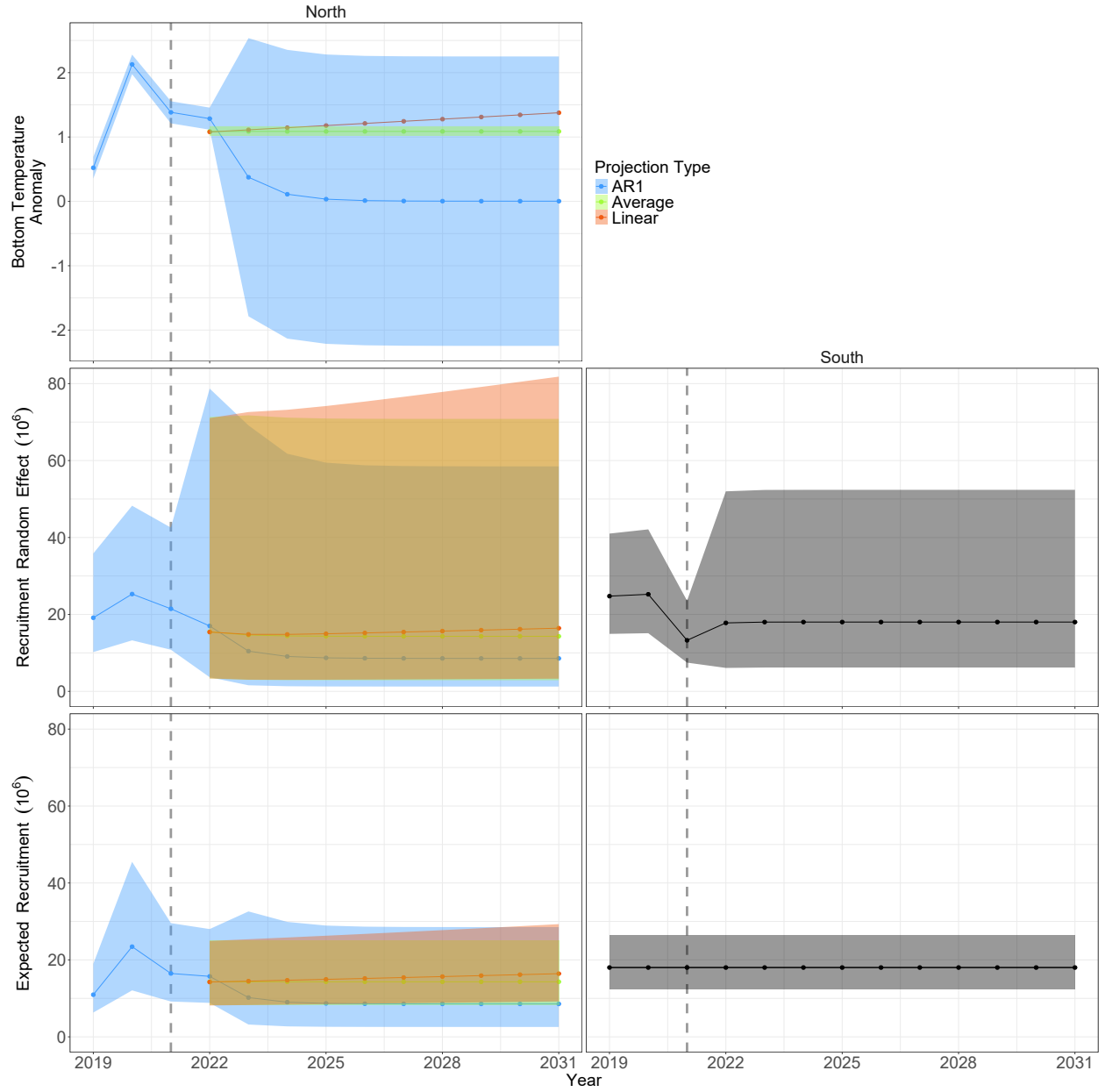


Figure 7: Annual estimates of bottom temperature in the northern region and alternative recruitment estimates (random effect or expected) by region. Estimates from years after 2021 are from projections of model $M1$ under three alternative assumptions for the bottom temperature anomalies in the northern region. Vertical dotted line is the last year of data and polygons represent 95% confidence intervals.

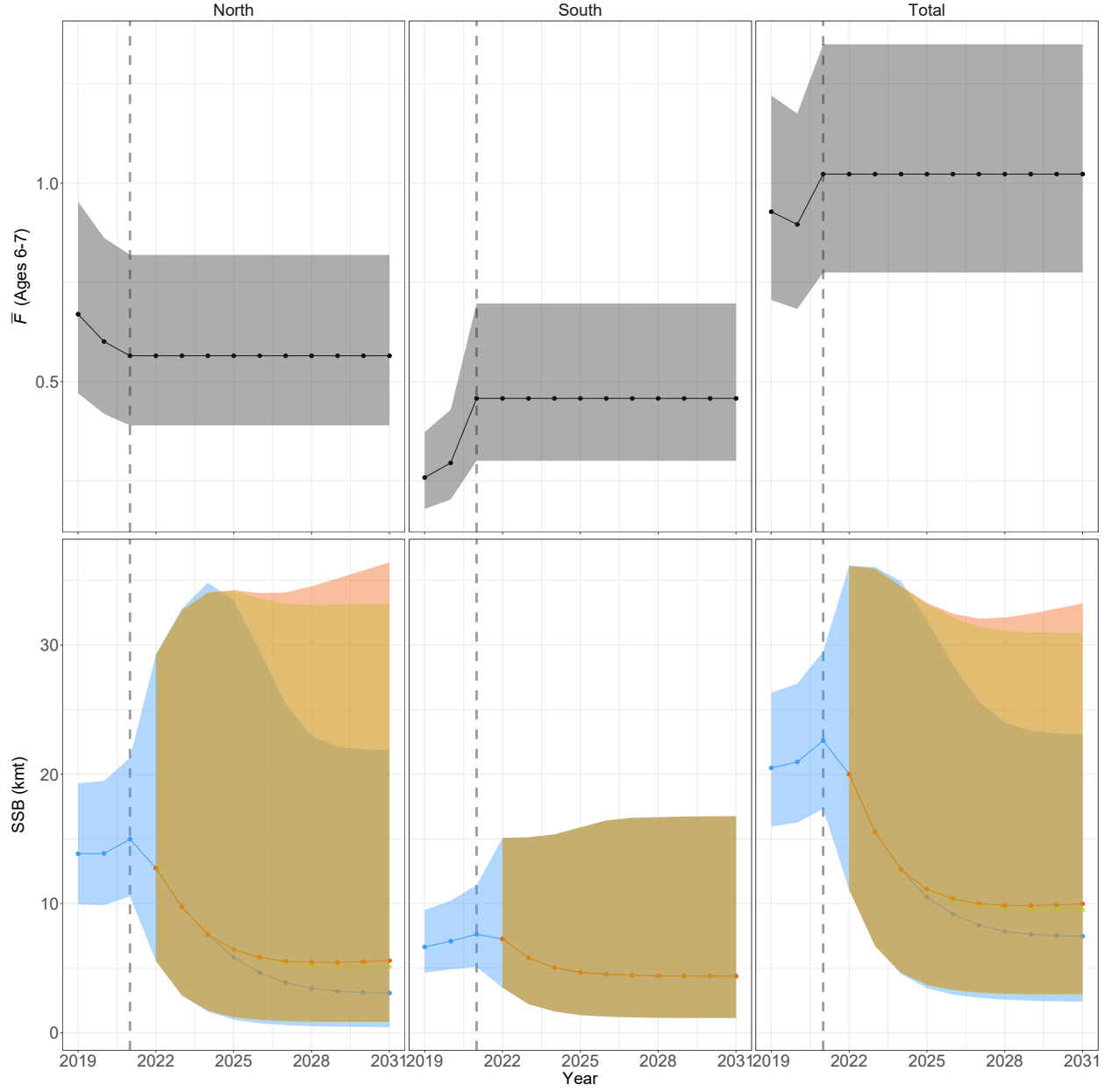


Figure 8: Annual estimates of average fishing mortality and SSB by region and in total. Estimates in years beyond 2021 are from projecting model M_1 under alternative assumptions for bottom temperature anomalies in the northern region. Vertical dotted line is the last year of data and polygons represent 95% confidence intervals.

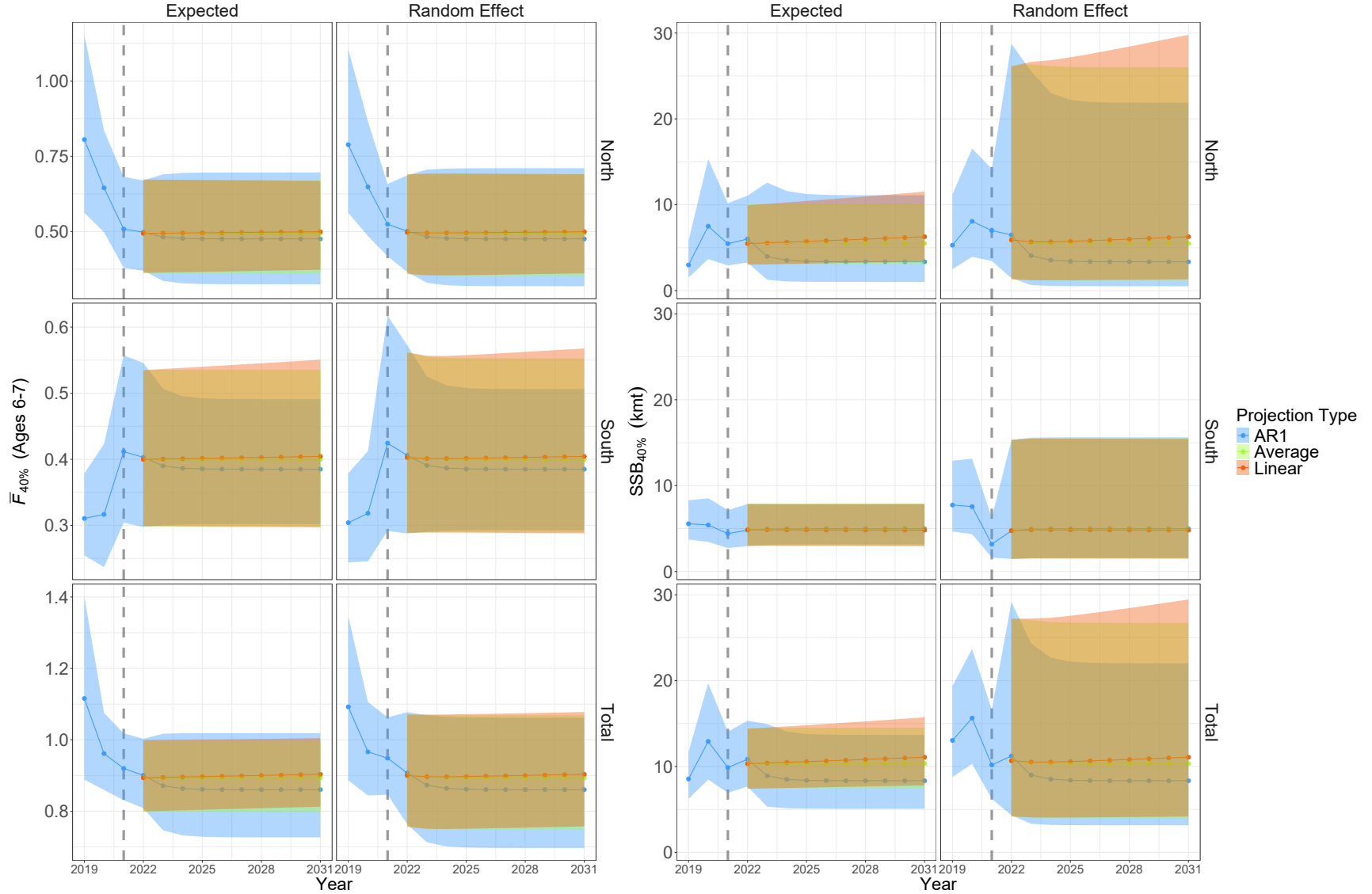


Figure 9: Annual estimates by region and in total of average equilibrium F at ages 6 and 7 that produces the 40% spawning potential ratio and SSB at $F_{40\%}$. Estimates in years beyond 2021 are from projecting model M_1 under alternative assumptions for bottom temperature anomalies in the northern region and average $\phi(\bar{F})$ inputs from the last 5 years of the unprojected model. Vertical dotted line is the last year of data and polygons represent 95% confidence intervals.

Tables

Table 1: Assumptions for temperature effects and random effects for age 1 natural mortality for each model.

Model	Temperature Effect		M at age 1 random effects
	North	South	
M_0	–	–	none
M_1	Recruitment	–	none
M_2	–	Recruitment	none
M_3	Recruitment	Recruitment	none
M_4	M at age 1	–	none
M_5	–	M at age 1	none
M_6	M at age 1	M at age 1	none
M_7	–	–	time-varying
M_8	Recruitment	–	time-varying
M_9	–	Recruitment	time-varying
M_{10}	Recruitment	Recruitment	time-varying
M_{11}	M at age 1	–	time-varying
M_{12}	–	M at age 1	time-varying
M_{13}	M at age 1	M at age 1	time-varying

Table 2: Difference between AIC and the lowest AIC for each model by retrospective peel.

Model	Peel							
	0	1	2	3	4	5	6	7
M_0	11.83	11.39	10.41	10.05	9.86	9.41	8.47	8.22
M_1	0.00	0.00	0.00	0.00	0.00	0.00	0.00	0.00
M_2	12.63	12.03	11.41	11.06	10.91	10.34	9.20	9.22
M_3	0.80	0.64	1.00	1.01	1.05	0.93	0.73	1.00
M_4	13.81	13.35	12.26	11.82	11.71	11.18	10.08	9.85
M_5	13.25	12.55	11.68	11.21	11.07	10.41	9.86	9.71
M_6	15.22	14.51	13.52	12.97	12.91	12.17	11.46	11.33
M_7	14.32	13.75	12.17	11.30	11.43	10.55	9.71	9.42
M_8	2.25	2.10	1.47	0.96	1.29	0.91	0.98	0.99
M_9	15.12	14.39	13.17	12.31	12.48	11.49	10.44	10.43
M_{10}	3.05	2.74	2.47	1.97	2.34	1.84	1.71	1.99
M_{11}	16.29	15.74	14.17	13.30	13.43	12.55	11.68	11.39
M_{12}	15.73	14.91	13.43	12.46	12.64	11.55	11.10	10.92
M_{13}	17.70	16.91	15.43	14.46	14.64	13.55	13.07	12.88

Table 3: Mohn's ρ for SSB, and average F at ages 6 and 7 in northern and southern regions.

Model	SSB		Average F	
	North	South	North	South
M_0	-0.040	-0.023	0.041	-0.048
M_1	-0.040	-0.023	0.041	-0.048
M_2	-0.040	-0.024	0.041	-0.047
M_3	-0.040	-0.024	0.041	-0.047
M_4	-0.041	-0.022	0.042	-0.048
M_5	-0.041	-0.023	0.042	-0.048
M_6	-0.042	-0.023	0.042	-0.048
M_7	-0.042	-0.022	0.043	-0.048
M_8	-0.044	-0.023	0.044	-0.048
M_9	-0.042	-0.024	0.043	-0.048
M_{10}	-0.044	-0.024	0.044	-0.047
M_{11}	-0.041	-0.022	0.042	-0.048
M_{12}	-0.042	-0.023	0.043	-0.048
M_{13}	-0.041	-0.023	0.042	-0.048

Table 4: Estimates of temperature effects on recruitment and variance and autocorrelation parameters for recruitment for northern (N) and southern (S) components for models with no effects (M_0), effects on specific components (M_1 and M_2) or both components simultaneously (M_3) from the full model (Peel 0) and each retrospective peel.

Parameter	Peel							
	0	1	2	3	4	5	6	7
$M_1 \hat{\beta}_{R,N}$	0.474	0.480	0.485	0.476	0.464	0.468	0.439	0.445
$M_2 \hat{\beta}_{R,S}$	0.099	0.105	0.094	0.095	0.092	0.096	0.099	0.091
$M_3 \hat{\beta}_{R,N}$	0.474	0.480	0.485	0.476	0.464	0.468	0.439	0.445
$M_3 \hat{\beta}_{R,S}$	0.099	0.105	0.094	0.095	0.092	0.096	0.099	0.091
M_0 Conditional $\hat{\sigma}_{R,N}$	0.925	0.953	0.978	0.988	0.978	1.010	0.981	1.007
M_1 Conditional $\hat{\sigma}_{R,N}$	0.730	0.752	0.780	0.786	0.775	0.801	0.785	0.800
$M_0 \hat{\rho}_{R,N}$	0.362	0.375	0.385	0.405	0.424	0.432	0.427	0.431
$M_1 \hat{\rho}_{R,N}$	0.296	0.307	0.334	0.373	0.394	0.406	0.428	0.429
M_0 Marginal $\hat{\sigma}_{R,N}$	0.992	1.028	1.060	1.080	1.081	1.120	1.084	1.117
M_1 Marginal $\hat{\sigma}_{R,N}$	0.764	0.791	0.827	0.848	0.843	0.877	0.869	0.885

Appendix A

Table A1: Definition of terms.

i	Seasonal time interval
δ_i	Length of seasonal time interval i
a	Age class
y	Year
A	Last age class (“plus group”)
r	Region
f	Fishing fleet
n_F	Number of fishing fleets
s	Stock
n_R	Number of regions
$\mathbf{P}_{y,a,i}$	Probability transition matrix for year y , age a , and season i
$\mathbf{O}_{y,a,i}$	submatrix of $\mathbf{P}_{y,a,i}$ of probabilities of surviving and occurring in each region for year y , age a , and season i
$\mathbf{H}_{y,a,i}$	submatrix of $\mathbf{P}_{y,a,i}$ of probabilities of being captured in each fishing fleet for year y , age a , and season i
\mathbf{I}_H	$n_f \times n_f$ identity matrix
m	Index observation
$O_{y,a,i}(r, r')$	For year y , age a and season i , the probability of surviving and occurring in region r' given beginning the interval alive in region r
$H_{y,a,i}(r, f)$	For year y , age a and season i , the probability of being captured in fleet f given beginning the interval alive in region r
$S_{y,a,i}$	For year y , age a and season i , the probability of surviving the interval (1 region model)
$F_{y,a,i,f}$	Fishing mortality rate for fleet f in year y at age a in seasonal interval i
$M_{y,a}$	Natural mortality rate in year y at age a (single region)
$M_{y,a,r}$	Natural mortality rate in region r and year y at age a
$Z_{y,a,i}$	Total mortality rate in year y at age a in seasonal interval i (single region)
$Z_{y,a,i,r}$	Total mortality rate in region r and year y at age a in seasonal interval i
$\mathbf{S}_{y,a,i}$	matrix of of probabilities of surviving in each region over the interval for season i , year y , age a

Table A1: (Continued)

$\mu_{y,a,i}$	matrix of probabilities of moving or staying in each region at the end of season i in year y and age a
$\mu_{r \rightarrow r',y,a,i}$	For year y , age a and seasonal interval i , either the probability of moving at the end of the interval or instantaneous rate of movement from region r to region r'
r_f	region where fleet f operates
$\mathbf{N}_{y,a}$	Column vector of abundances by region at age a in year y
$\mathbf{A}_{y,a,i}$	instantaneous rate matrix for seasonal interval i , year y , and age a
$a_{y,a,i,r}$	For year y , age a and seasonal interval i , the hazard or negative sum of the instantaneous rates of mortality and movement from the state corresponding to being alive in region r
$\mathbf{P}_{y,a}(\delta_1, \dots, \delta_K)$	Probability transition matrix for year y and age a over seasonal intervals $\delta_1, \dots, \delta_K$
K	Number of seasons in the annual time step
t_s	fraction of the annual time step when spawning occurs for stock s
$\delta_{s,i}$	fraction of the annual time step between t_s and the beginning of season i
t_m	fraction of the annual time step when index m observes the population
$\delta_{m,i}$	fraction of the annual time step between t_m and the beginning of season i
$\mathbf{N}_{y,a}$	Abundance at age a in year y in each of the living and mortality states on January 1
$\mathbf{N}_{O,y,a}$	Abundance at age a in year y alive in each region on January 1
$N_{y,a,r}$	Abundance at age a in year y alive in region r on January 1
r_s	region where stock s spawns and recruits
SSB_{y,r_s}	Spawning stock biomass for a given stock in region r_s in year y
$\varepsilon_{y,a,r}$	Random error for abundance at age a in year y in region r
$w_{y,a}$	mean individual weight for a given stock at age a in year y
$\text{mat}_{y,a}$	proportion mature at age a in year y for a given stock
$\mathbf{O}_{y,a,r_s}(t_s)$	Probabilities of surviving and occurring in region r_s at time t_s given being alive in each region at the start of the year
$\boldsymbol{\varepsilon}_{y,a}$	vector of random errors for abundance alive in each region on January 1 of year y at age a
$\sigma_{N,r}$	standard deviation parameter for abundance at age random effects in region r
$\rho_{N,\text{age},r}$	first order auto-regressive correlation parameter across age for abundance at age random effects in region r
$\rho_{N,\text{year},r}$	first order auto-regressive correlation parameter across year for abundance at age random effects in region r

Table A1: (Continued)

$\text{sel}_{1,a,f}$	selectivity scalar at age a for fleet f in the first year
$F_{1,a,f}$	fishing mortality rate at age a for fleet f in the first year
$\tilde{F}_{a,f}$	equilibrium fishing mortality rate at age a for fleet f
\mathbf{O}_a	proportion surviving the year at age a and occurring in each region (columns) given alive on January 1 in each region (rows)
$\tilde{\mathbf{O}}_a$	equilibrium proportions alive in each region at age a (columns) given recruitment in each region (rows)
$\mathbf{N}_{O,1,r}$	vector of abundance by age in region r in the first year
$\theta_{N_1,r}$	mean parameter for initial numbers at age random effects in the first year for region r
$\boldsymbol{\varepsilon}_{N_1,r}$	vector of random effects by age for initial numbers at age in the first year for region r
$\sigma_{N_1,r}$	standard deviation parameter for initial numbers at age random effects in the first year for region r
$\rho_{N_1,r}$	first order auto-regressive correlation parameter for initial numbers at age random effects in the first year for region r
$\mu_{r \rightarrow r',y,a,i}$	movement rate from region r to region r' in seasonal interval i and year y at age a
$g(\mu_{r \rightarrow r',y,a,i})$	link function for movement rate $\mu_{r \rightarrow r',y,a,i}$
$\theta_{r \rightarrow r',i}$	mean or intercept parameter across age and year for movement from region r to region r' in seasonal interval i
$\varepsilon_{r \rightarrow r',y,a,i}$	random effect for movement from region r to region r' in seasonal interval i and year y at age a
n_E	number of environmental covariates
$\beta_{r \rightarrow r',a,i,k}$	effect of environmental covariate k on movement from region r to r' at age a in seasonal interval i
$E_{k,y}$	latent environmental covariate k affecting the population in year y
$\sigma_{r \rightarrow r',i}$	standard deviation parameter for movement random effects from region r to r' in seasonal interval i
$\rho_{r \rightarrow r',\text{age},i}$	first order auto-regressive correlation parameter across age for movement random effects from region r to r' in seasonal interval i
$\rho_{r \rightarrow r',\text{year},i}$	first order auto-regressive correlation parameter across year for movement random effects from region r to r' in seasonal interval i

Table A1: (Continued)

$\gamma_{r \rightarrow r', i}$	random effect for link-transformed mean movement from region r to r' in seasonal interval i when a prior distribution is assumed
$\sigma_{r \rightarrow r', i}$	standard deviation parameter for prior distribution of $\gamma_{r \rightarrow r', i}$
$M_{y, a, r}$	natural mortality rate for age a in year y in region r
$\theta_{M, r}$	mean parameter across age and year for natural mortality in region r
$\varepsilon_{M, r, y, a}$	random effect parameter for natural mortality in region r and year y at age a
$\beta_{M, r, a, k}$	effect of environmental covariate k on natural mortality in region r at age a
$\sigma_{M, r}$	standard deviation parameter for natural mortality random effects in region r
$\rho_{M, \text{age}, r}$	first order auto-regressive correlation parameter across age for natural mortality random effects in region r
$\rho_{M, \text{year}, r}$	first order auto-regressive correlation parameter across year for natural mortality random effects in region r
$\hat{\mathbf{N}}_{H, s, y, a}$	vector of predicted numbers of stock s at age a in year y captured by each fleet
$\hat{\mathbf{N}}_{H, y, a}$	vector of predicted numbers at age a in year y captured by each fleet across all stocks
$\hat{\mathbf{C}}_{y, a}$	vector of predicted biomass captured at age a in year y by each fleet across all stocks
$\mathbf{c}_{y, a}$	vector of mean individual weight at age a in year y for each fleet
$\hat{\mathbf{C}}_y$	vector of predicted aggregate catch for each fleet in year y
$C_{y, f}$	observed aggregate catch for fleet f in year y
$\hat{C}_{y, f}$	predicted aggregate catch for fleet f in year y
$\sigma_{y, f}$	standard deviation of observed log-aggregate catch for fleet f in year y
$\hat{N}_{s, y, a, m}$	predicted abundance at t_m in region r_m
$\mathbf{O}_{s, y, a, r_m}(t_m)$	the probabilities of surviving and occurring in region r_m at time t_m given being alive in each region at the start of the year which is the r_m column of the upper-left submatrix of Eq. 4
$\hat{I}_{m, y, a}$	Predicted relative abundance index for survey d in year y at age a
$q_{m, y}$	catchability of index m in year y
$\text{sel}_{m, y, a}$	selectivity of index m at age a in year y
$w_{m, y, a}$	average weight of individuals at age a for index m if the index is quantified in biomass, otherwise it is unity
u_m	upper bound for index m catchability
l_m	lower bound for index m catchability
$\theta_{q, m}$	mean index m catchability parameter

Table A1: (Continued)

$\varepsilon_{q,m,y}$	index m catchability random effect in year y
$\beta_{q,m,k}$	effect of environmental covariate k on index m catchability
$\sigma_{q,r}$	standard deviation parameter for index m catchability random effects
$\rho_{q,m}$	first order auto-regressive correlation parameter across year for index m catchability random effects
$\text{sel}_{f,a}$	selectivity of fleet f at age a for SPR-based reference points
$\bar{F}_{f,a}$	Average fishing mortality for fleet f at age a over user-specified set of years
$\phi(\tilde{F})$	equilibrium spawning biomass per recruit for stock s at fully-selected fishing mortality rate \tilde{F}
$\tilde{\mathbf{O}}_{a,r_s,\cdot}$	proportion surviving the year at age a and occuring in each region (columns) given alive on January 1 in region r_s
$\mathbf{O}_{a,\cdot,r_s}(t_s)$	proportion surviving the year at age a starting in each region (rows) and occuring in region r_s at spawning time t_s
$\tilde{\nu}(\tilde{F})$	matrix of equilibrium yield per recruit by region and fleet at fully-selected fishing mortality rate \tilde{F}
λ_s	weight for stock s to use for spawning biomass per recruit for defining SPR-based fishing mortality reference point

Appendix B

New features of WHAM 2.0 that are not used in the application to black sea bass are described here..

Simultaneous movement and mortality

When survival and movement are assumed to occur simultaneously, all movement and mortality parameters are instantaneous rates. We obtain the PTM over an interval i by exponentiating the instantaneous rate matrix (Miller and Andersen 2008)

$$\mathbf{P}_{y,a,i} = e^{\mathbf{A}_{y,a,i}\delta_i}$$

The instantaneous rate matrix takes rates of movement between regions and the mortality rates for each fleet and region. Along the diagonal is the negative of the sum of the other rates (the hazard) so each row

857 sums to zero. For two regions and one fleet operating in each region:

$$\mathbf{A}_{y,a,i} = \begin{bmatrix} a_{y,a,i,1} & \mu_{1 \rightarrow 2,y,a,i} & F_{y,a,i,1} & 0 & M_{y,a,1} \\ \mu_{2 \rightarrow 1,y,a,i} & a_{y,a,i,2} & 0 & F_{y,a,i,2} & M_{y,a,2} \\ 0 & 0 & 0 & 0 & 0 \\ 0 & 0 & 0 & 0 & 0 \\ 0 & 0 & 0 & 0 & 0 \end{bmatrix}$$

858 where $a_{y,a,i,r} = -(\mu_{r \rightarrow r',y,a,i} + F_{y,a,i,r} + M_{y,a,r})$. When there is one region, n_f fleets, and $\delta_i = 1$, exponen-
859 tiating the instantaneous rate matrix results in the PTM defined in Eq. 2.

860 Initial abundance at age as random effects

861 The initial abundances at age can also be treated as independent or AR1 random effects. Defining the vector
862 of initial abundance at age in region r as $\mathbf{N}_{O,1,r}$, the general model is

$$\log \mathbf{N}_{O,1,r} = \theta_{N_1,r} + \varepsilon_{N_1,r}$$

863 where

$$Cov(\varepsilon_{N_1,a,r}, \varepsilon_{N_1,a',r}) = \frac{\rho_{N_1,r}^{|a-a'|} \sigma_{N_1,r}^2}{(1 - \rho_{N_1,r}^2)}.$$

864 General natural mortality model

865 The general model for natural mortality at age a for a given stock in region r is a function of random and
866 covariate effects

$$\log M_{y,a,r} = \theta_{M,r} + \varepsilon_{M,r,y,a} + \sum_{k=1}^{n_E} \beta_{M,r,a,k} E_{k,y}.$$

867 The general covariance structure for random effects are modeled most generally as 2DAR1 random effect
868 with age and(or) year where the covariance is

$$Cov(\varepsilon_{M,y,a,r}, \varepsilon_{M,y',a',r}) = \frac{\rho_{M,\text{age},r}^{|a-a'|} \rho_{M,\text{year},r}^{|y-y'|} \sigma_{M,r}^2}{(1 - \rho_{M,\text{age},r}^2) (1 - \rho_{M,\text{year},r}^2)}.$$

869 General catchability model

870 Catchability of each index can be treated as logit functions of normal random effects and(or) environmental
871 covariate effects

$$\log \frac{q_{m,y} - l_m}{u_m - q_{m,y}} = \theta_{q,m} + \varepsilon_{q,m,y} + \sum_{k=1}^{n_E} \beta_{q,m,k} E_{k,y}$$

872 where $\theta_{q,m}$ is an intercept or mean parameter, and u_m and l_m are the upper and lower bounds of catchability
873 for index m (defaults are 0 and 1000). The general covariance structure for the annual random effects is

874 AR1

$$Cov(\varepsilon_{q,m,y}, \varepsilon_{q,m,y'}) = \frac{\rho_{q,m}^{|y-y'|} \sigma_{q,m}^2}{1 - \rho_{q,m}^2}.$$

Supplementary Materials

Deriving the prior distribution for movement parameters

The Working Group fit a Stock Synthesis model (Methot and Wetzel 2013) that included tagging data with 2 seasons (6 months each) and 2 regions where a proportion μ_1^* of the northern component moves to the south in one season and some proportion $\mu_{2 \rightarrow 1}^*$ move back to the south in the second season (NEFSC 2023). The seasonal movement matrices for each season are

$$\boldsymbol{\mu}_1^* = \begin{bmatrix} 1 - \mu_{1 \rightarrow 2}^* & \mu_{1 \rightarrow 2}^* \\ 0 & 1 \end{bmatrix}$$

and

$$\boldsymbol{\mu}_2 = \begin{bmatrix} 1 & 0 \\ \mu_{2 \rightarrow 1}^* & 1 - \mu_{2 \rightarrow 1}^* \end{bmatrix}.$$

To obtain estimates of movement proportions for the monthly intervals in the WHAM model, the half-year movement matrices were converted to monthly movement matrices by taking the root z_k of $\boldsymbol{\mu}_k^*$ which are defined by the number of months of movement for each season (5 and 4, respectively). The roots of the matrices are calculated using an eigen decomposition of the matrices

$$\boldsymbol{\mu}_k = (\boldsymbol{\mu}_k^*)^{z_k} = \mathbf{V}_k \mathbf{D}_k^{z_k} \mathbf{V}_k^{-1}$$

where $z_1 = 1/5$ for and $z_2 = 1/4$, and \mathbf{V}_k and \mathbf{D}_k are the matrix of eigenvectors (columnwise) and the diagonal matrix of corresponding eigenvalues of $\boldsymbol{\mu}_k^*$. The Working Group used a parametric bootstrap approach to determine an appropriate standard deviation for the prior distribution for the movement parameters. Stock Synthesis also estimates parameters on a transformed scale, but different from WHAM:

$$\mu_{r \rightarrow r'}^* = \frac{1}{1 + 2e^{-x_{r \rightarrow r'}}}$$

The estimated parameters and standard errors from the Stock Synthesis model were $x_{1 \rightarrow 2} = -1.44$ and $x_{2 \rightarrow 1} = 1.94$ and $SE(x_{1 \rightarrow 2}) = 0.21$ and $SE(x_{2 \rightarrow 1}) = 0.37$. The resulting in the estimated proportions were $\mu_{1 \rightarrow 2}^* = 0.11$ and $\mu_{2 \rightarrow 1}^* = 0.78$.

In WHAM, an additive logit transformation is used which is simply a logit transformation when there are

only two regions:

$$\mu_{r \rightarrow r'} = \frac{1}{1 + e^{-y_{r \rightarrow r'}}}.$$

We simulated 1000 values from a normal distribution with mean and standard deviation defined by the parameter estimate and standard error $\tilde{x}_{r \rightarrow r', b} \sim N(x_{r \rightarrow r'}, SE(x_{r \rightarrow r'}))$ from the Stock Synthesis model. For each simulated value we constructed $\tilde{\mu}_{r \rightarrow r', b}^*$, took the appropriate root and calculated inverse logit for $\tilde{y}_{r \rightarrow r', b}$. We calculated the mean and standard deviation of the values $y_{i, b}$. The mean values did not differ meaningfully from the transformation of the original estimates ($y_{1 \rightarrow 2} = -3.79$ and $y_{2 \rightarrow 1} = -0.79$) and the standard deviation was approximately 0.2 for both parameters.

Bottom temperature anomalies

The Working Group created bottom temperature observations from a high resolution ocean bottom temperature product by du Pontavice et al. (2023). The annual observations for each region are defined by the average over all spatial bottom temperature values for February and March by region and year. Similarly, the Working Group calculated standard errors from the standard deviation of all values in the region and the total number of values for a given year. We created regional bottom temperature anomalies by subtracting means for each region across all years.

Diagnostics

Jitter fits for model M_0

WHAM by default completes three newton steps after the stats::nlminb minimization function completes to reduce the gradient at the minimized NLL. However, this generally has negligible effects on model estimates and the NLL. To reduce computation time, we did not complete these newton steps when performing jitter fits of the model. Without the Newton steps, the maximum (absolute) gradient sizes are generally less than 0.01 for models that converge satisfactorily.

The 50 jitter fits demonstrated that a local minimum was obtained for the original fit of model M_0 (Figure S1). One lower NLL was obtained with unacceptable gradients (No. 25), but a slightly lower NLL was found with a satisfactory gradient for 3 of the jitters (Nos. 9, 13, 29). However, one of the jitter fits (No. 9) did not provide a non-zero estimate of the variance parameter for one of the indices and the other two provided identical results and we refit model M_0 and all remaining models using the better parameter estimates as initial values.

Jitter fits for model M_1

The 50 jitter fits gave no evidence of a better minimization of the NLL. Three lower NLLs were obtained, but with unacceptably large gradients (Figure S2). The largest differences in parameter estimates for these three jitters were for numbers at age and selectivity random effects variance and correlation parameters.

Self test for model M_1

Initial fits to simulated data from model M_1 showed estimation of the observation error standard deviation multiplier for the recreational catch-per angler indices in the north and south regions was unstable. Many of the fits to the simulated data produced implausible estimates at the 0 boundary for these parameters (very negative values on log-scale). However, across all fits including those with poor convergence, estimation of SSB and fishing mortality was reliable (Figure S3). We also fit analogous models with the multiplier parameters fixed at the true values, which did improve convergence, but larger bias was estimated for fishing mortality and SSB for the northern component.

Table S1: Configuration of age composition likelihoods, mean selectivity models, and selectivity random effects models for each age composition data component. For all logistic-normal likelihoods, any ages observed as zeros are treated as missing.

Data component	Age Composition Likelihood	Mean Selectivity model	Random effects Model
North commercial fleet	Dirichlet-Multinomial	age-specific (ages > 3 fully selected)	AR1 correlation by age and year
North recreational fleet	Logistic-normal (Independent)	age-specific (ages > 6 fully selected)	AR1 correlation by age and year
South commercial fleet	Logistic-normal (AR1 correlation)	logistic	None
South recreational fleet	Logistic-normal (AR1 correlation)	logistic	None
North recreational CPA index	Logistic-normal (Independent)	age-specific (ages > 1 fully selected)	AR1 correlation by year
North VAST index	Dirichlet-Multinomial	age-specific (ages > 4 fully selected)	AR1 correlation by age and year
South recreational CPA index	Logistic-normal (AR1 correlation)	age-specific (ages > 2 fully selected)	None
South VAST index	Logistic-normal (AR1 correlation)	age-specific (ages > 1 fully selected)	None

Table S2: Model AIC weights for each retrospective peel.

Model	Peel							
	0	1	2	3	4	5	6	7
M_0	0.00	0.00	0.00	0.00	0.00	0.00	0.01	0.01
M_1	0.45	0.43	0.42	0.38	0.41	0.37	0.36	0.38
M_2	0.00	0.00	0.00	0.00	0.00	0.00	0.00	0.00
M_3	0.30	0.31	0.25	0.23	0.24	0.23	0.25	0.23
M_4	0.00	0.00	0.00	0.00	0.00	0.00	0.00	0.00
M_5	0.00	0.00	0.00	0.00	0.00	0.00	0.00	0.00
M_6	0.00	0.00	0.00	0.00	0.00	0.00	0.00	0.00
M_7	0.00	0.00	0.00	0.00	0.00	0.00	0.00	0.00
M_8	0.15	0.15	0.20	0.24	0.21	0.24	0.22	0.23
M_9	0.00	0.00	0.00	0.00	0.00	0.00	0.00	0.00
M_{10}	0.10	0.11	0.12	0.14	0.13	0.15	0.15	0.14
M_{11}	0.00	0.00	0.00	0.00	0.00	0.00	0.00	0.00
M_{12}	0.00	0.00	0.00	0.00	0.00	0.00	0.00	0.00
M_{13}	0.00	0.00	0.00	0.00	0.00	0.00	0.00	0.00

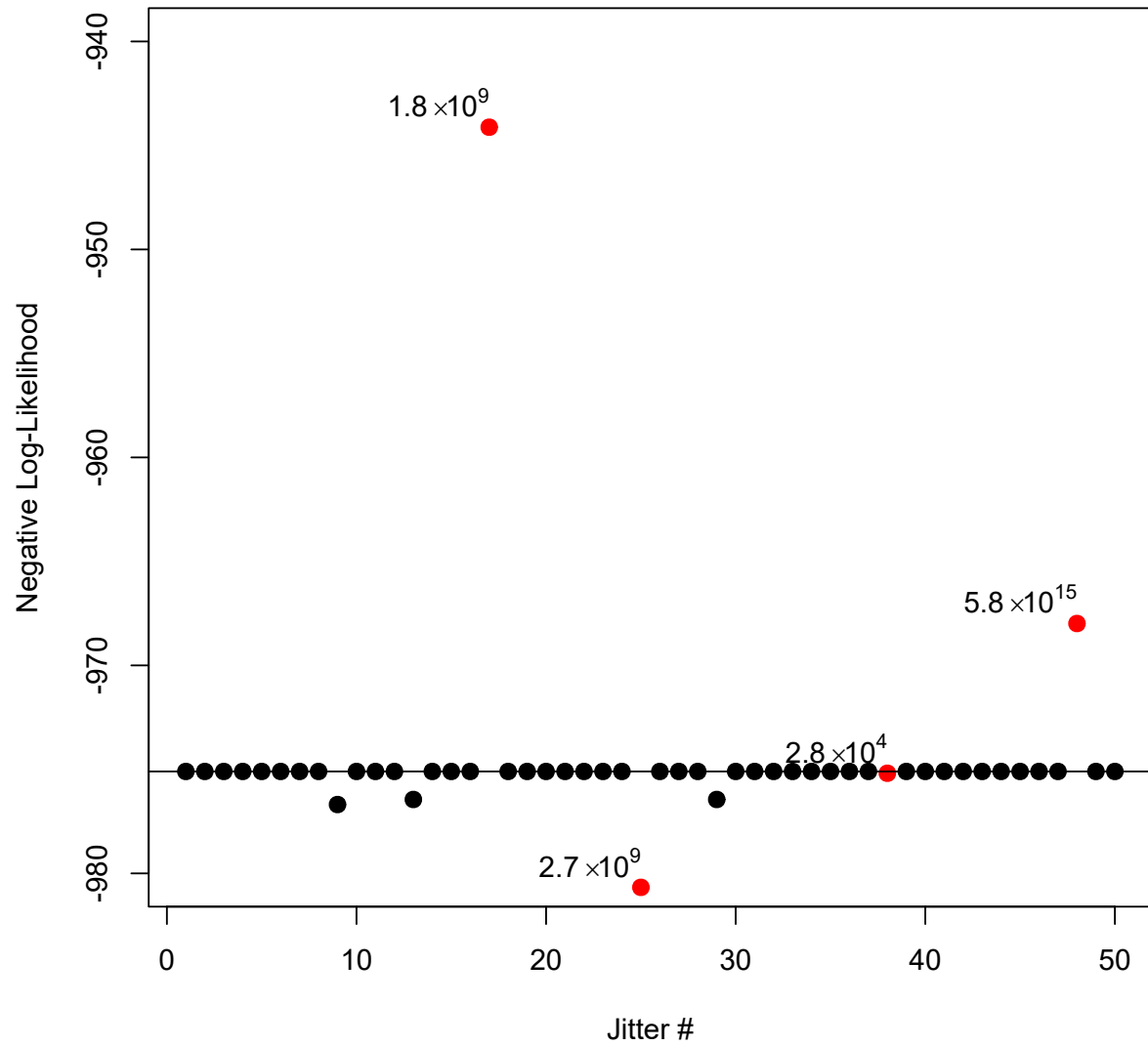


Figure S1: Minimized negative log-likelihood for 50 fits where minimization used initial parameter values jittered from those provided by an initial fit for model M_0 . Black jitters had maximum absolute gradient values $< 10^{-2}$ and red jitters had values > 1 .

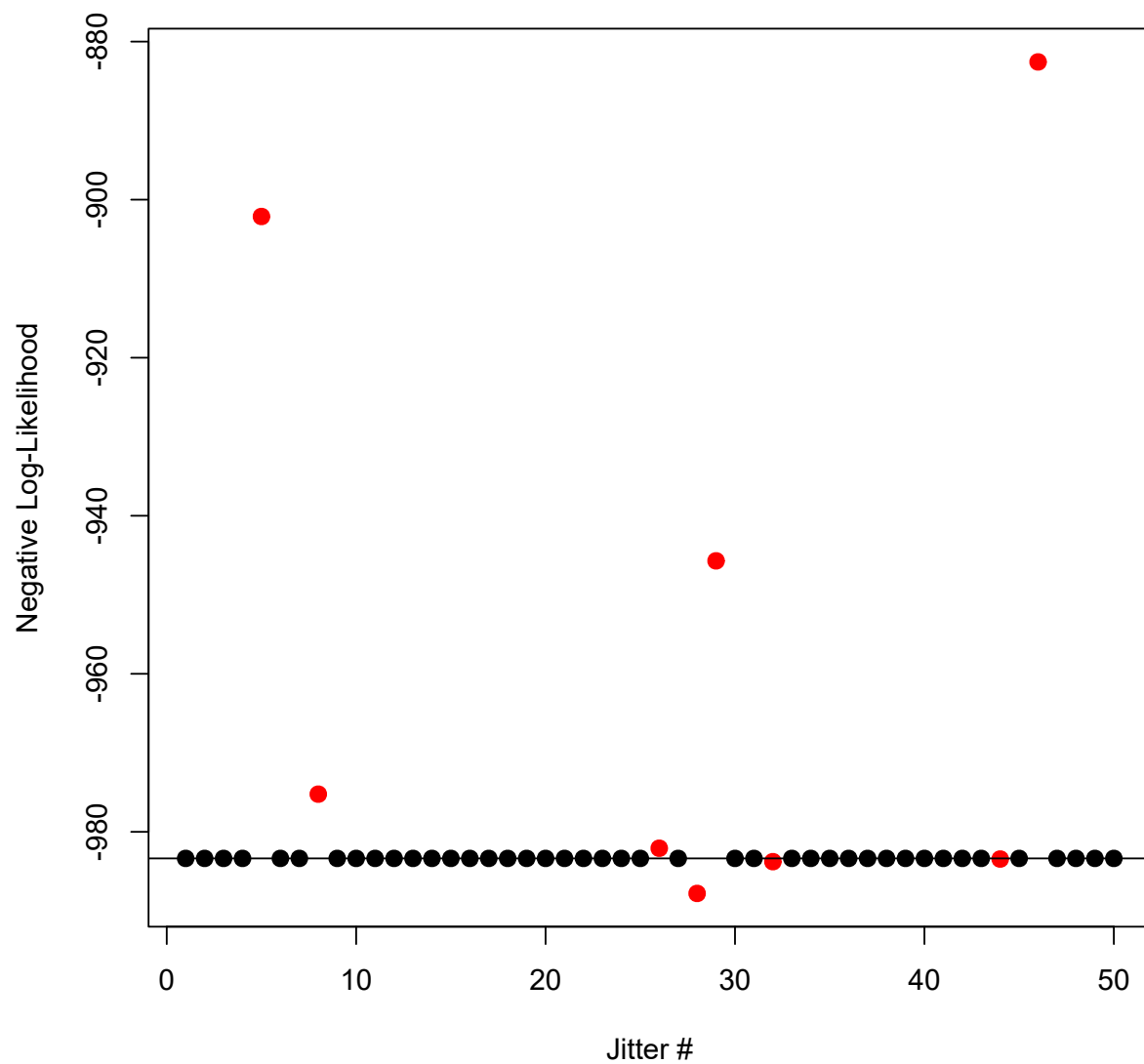


Figure S2: Minimized negative log-likelihood for 50 fits where minimization used initial parameter values jittered from those provided by an initial fit for model M_1 . Fits with black dots had maximum absolute gradient value < 0.01 and fits with red dots had values > 10 .

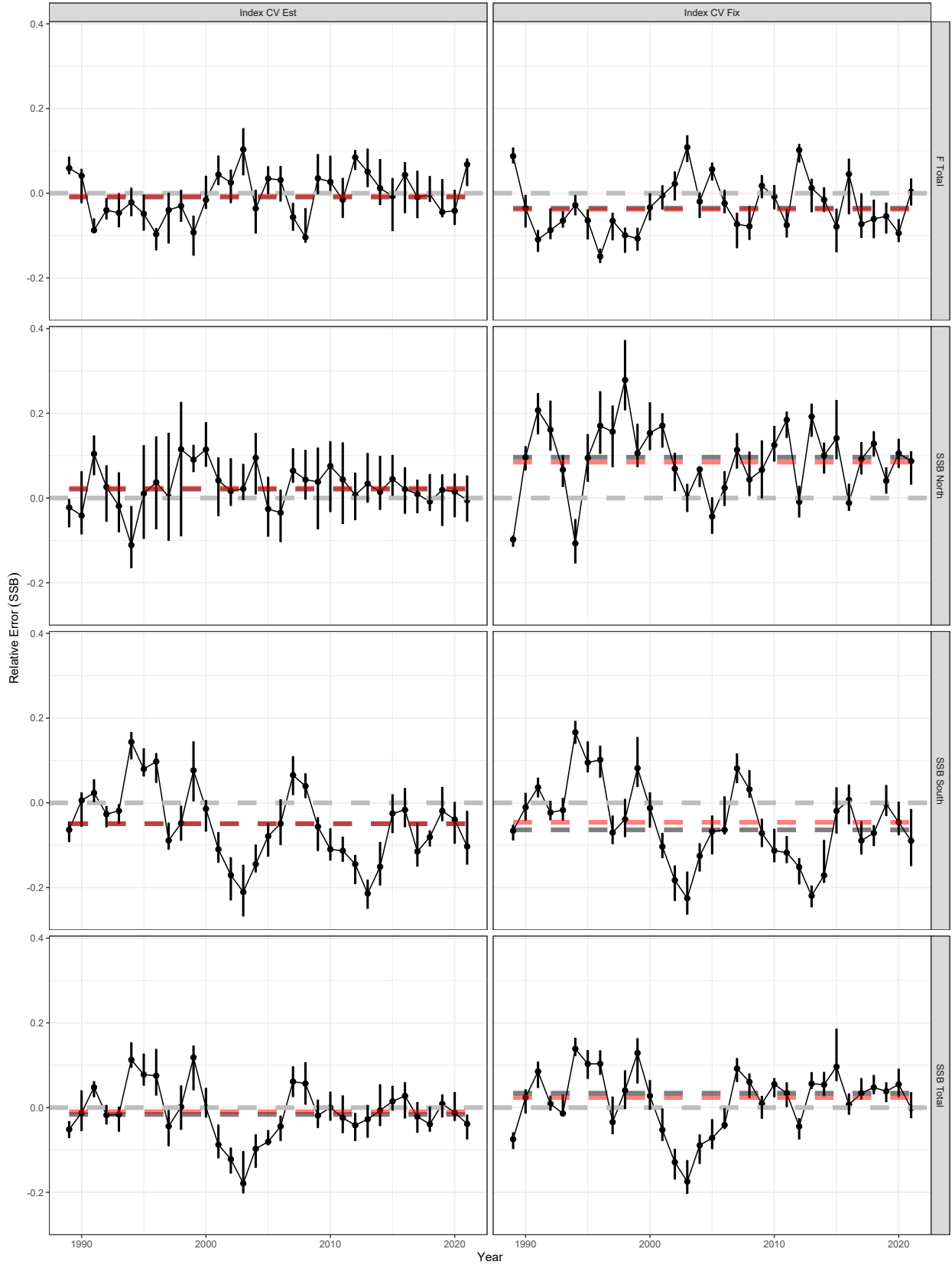


Figure S3: Median relative error of SSB (Total and by stock component) and total fully-selected fishing mortality for estimation models fitted to simulated data from model M_1 where the observation variance of log-indices are fixed and estimated. Black and Red dashed lines represent the median of the annual medians and the median across all annual relative errors, respectively. Vertical lines represent 95% confidence intervals.

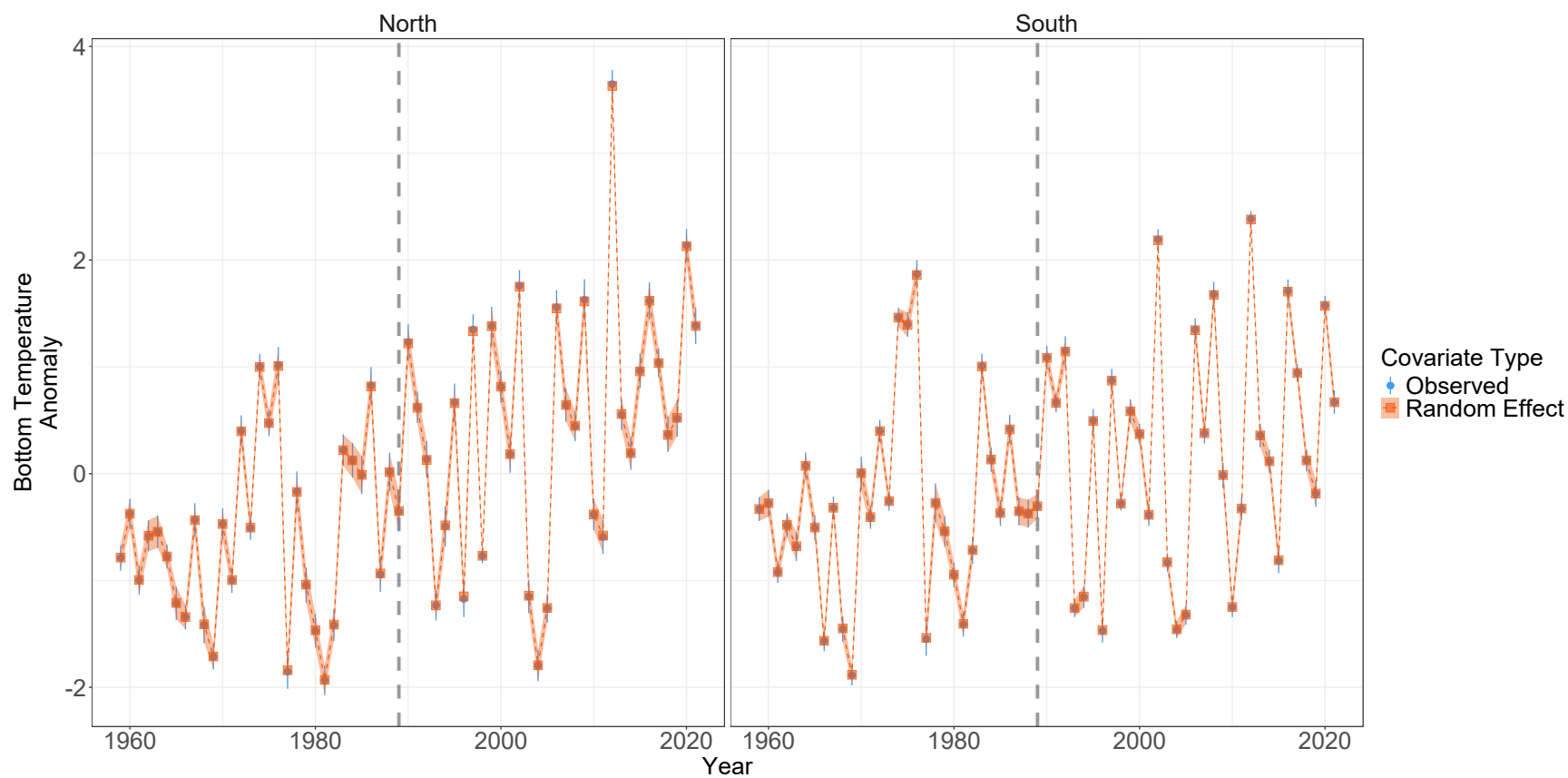


Figure S4: Observations with 95% confidence intervals (points with vertical lines) and posterior estimates with 95% confidence intervals (lines with polygons) of bottom temperature anomalies in the north and south regions from model M_1 . Gray vertical line defines the first year that the black sea bass stock is modeled.

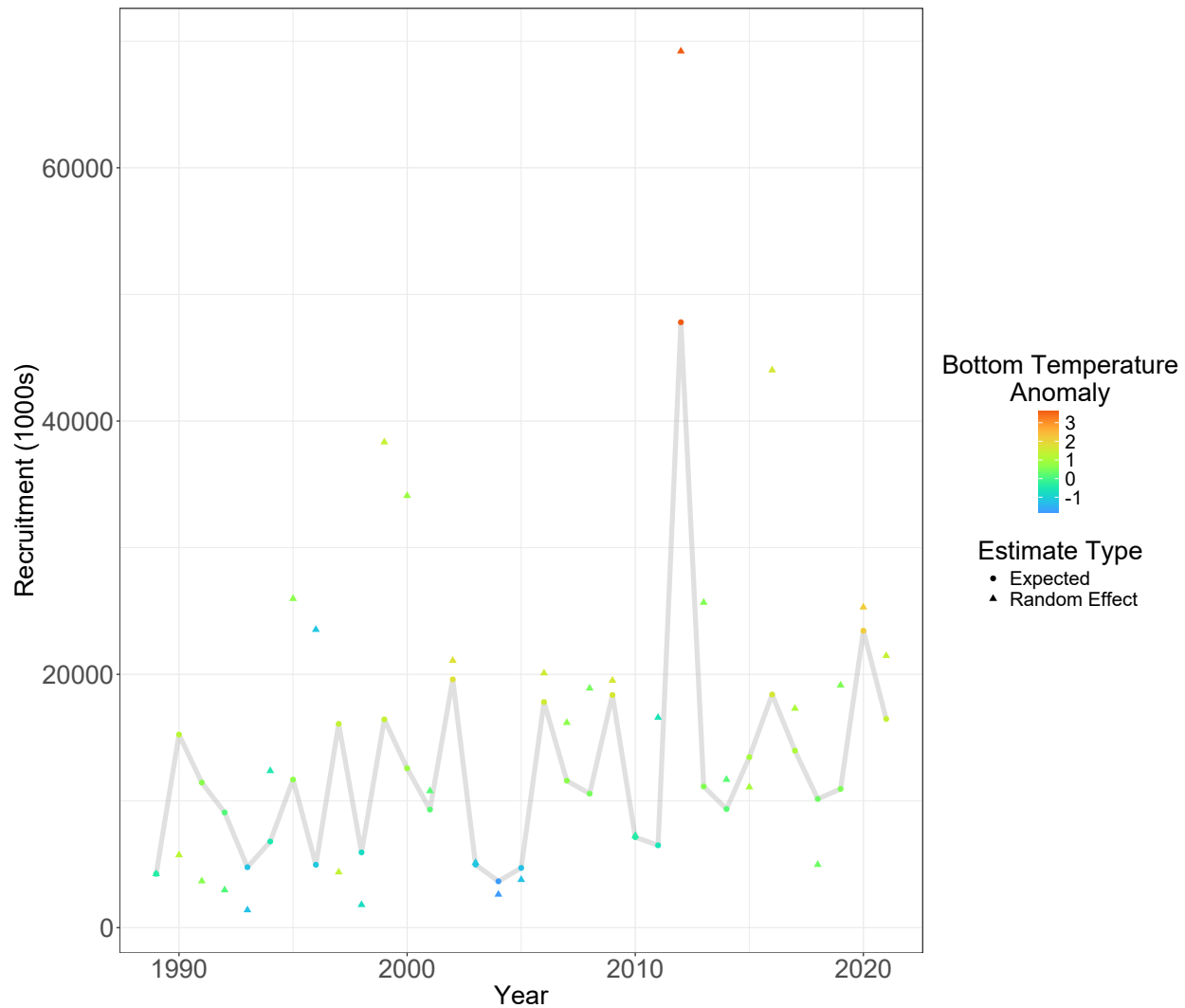


Figure S5: Expected and random effect recruitment estimates for the northern stock component. Color of points defined by the corresponding annual bottom temperature anomaly.

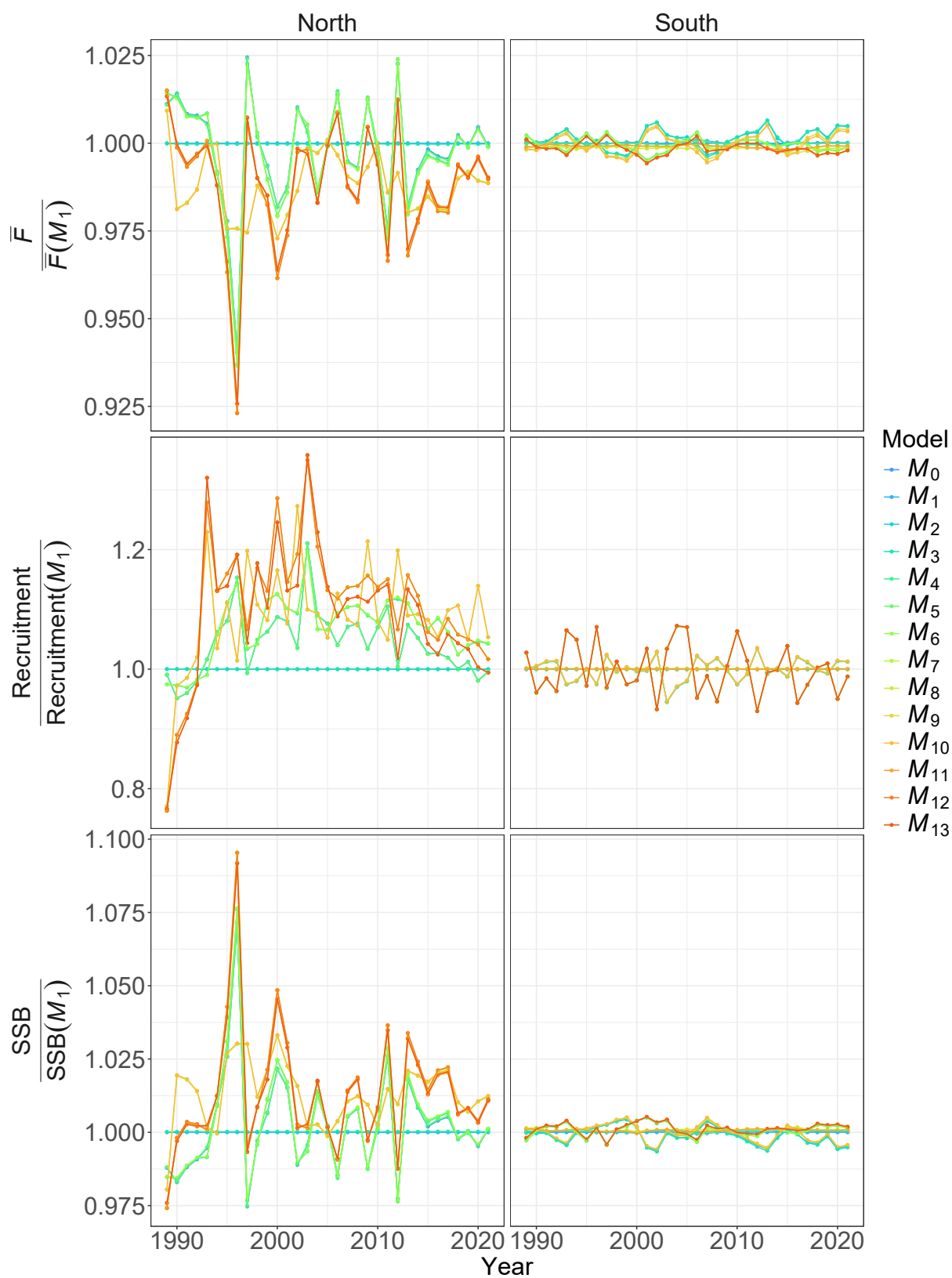


Figure S6: Estimates of SSB, F , and recruitment relative to those of the best performing model, M_1 .

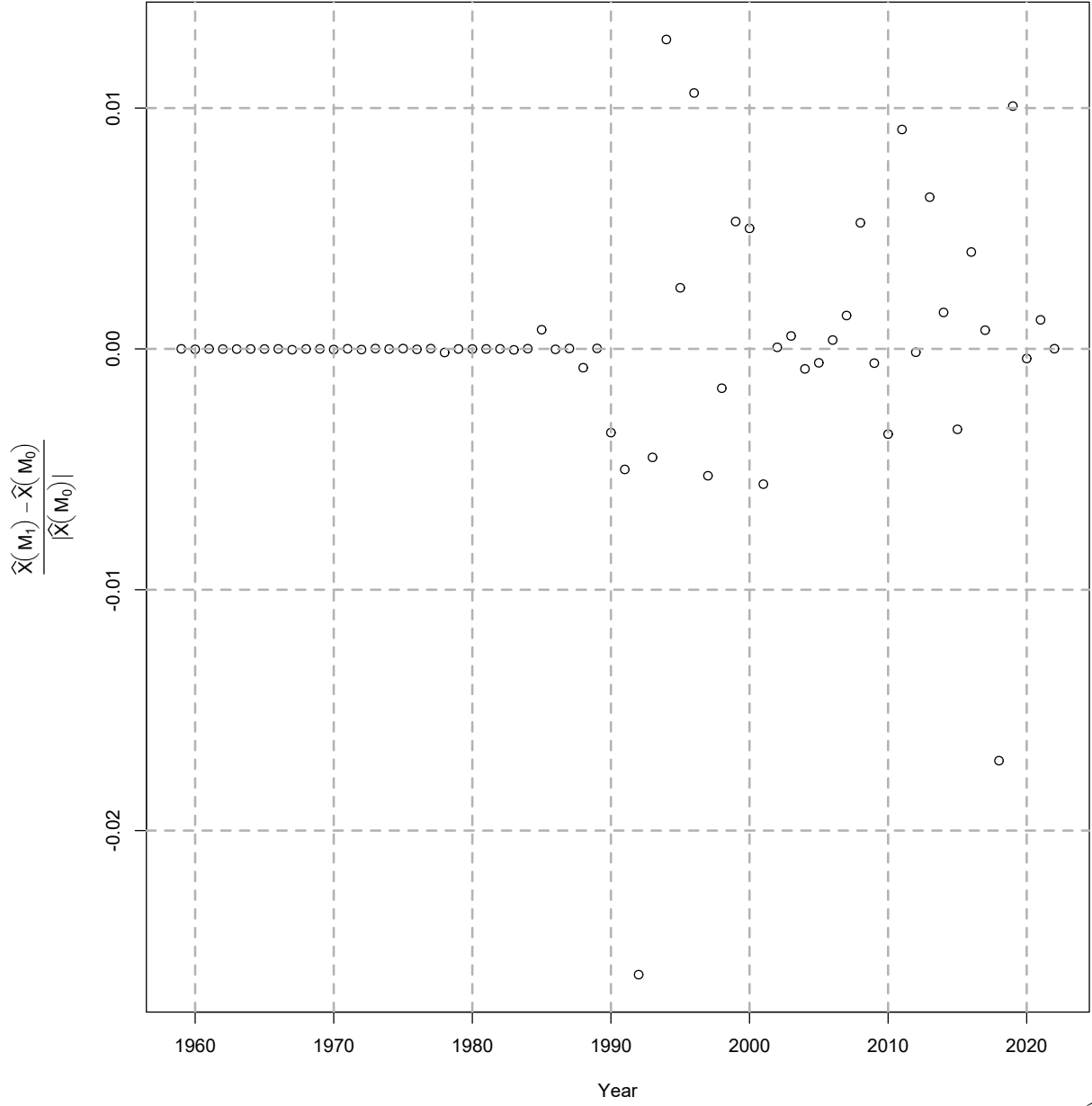


Figure S7: Relative differences in posterior estimates of northern region bottom temperature anomalies (\hat{X}) from the null model without effects on recruitment (M_0) and with effects on the northern stock component (M_1).

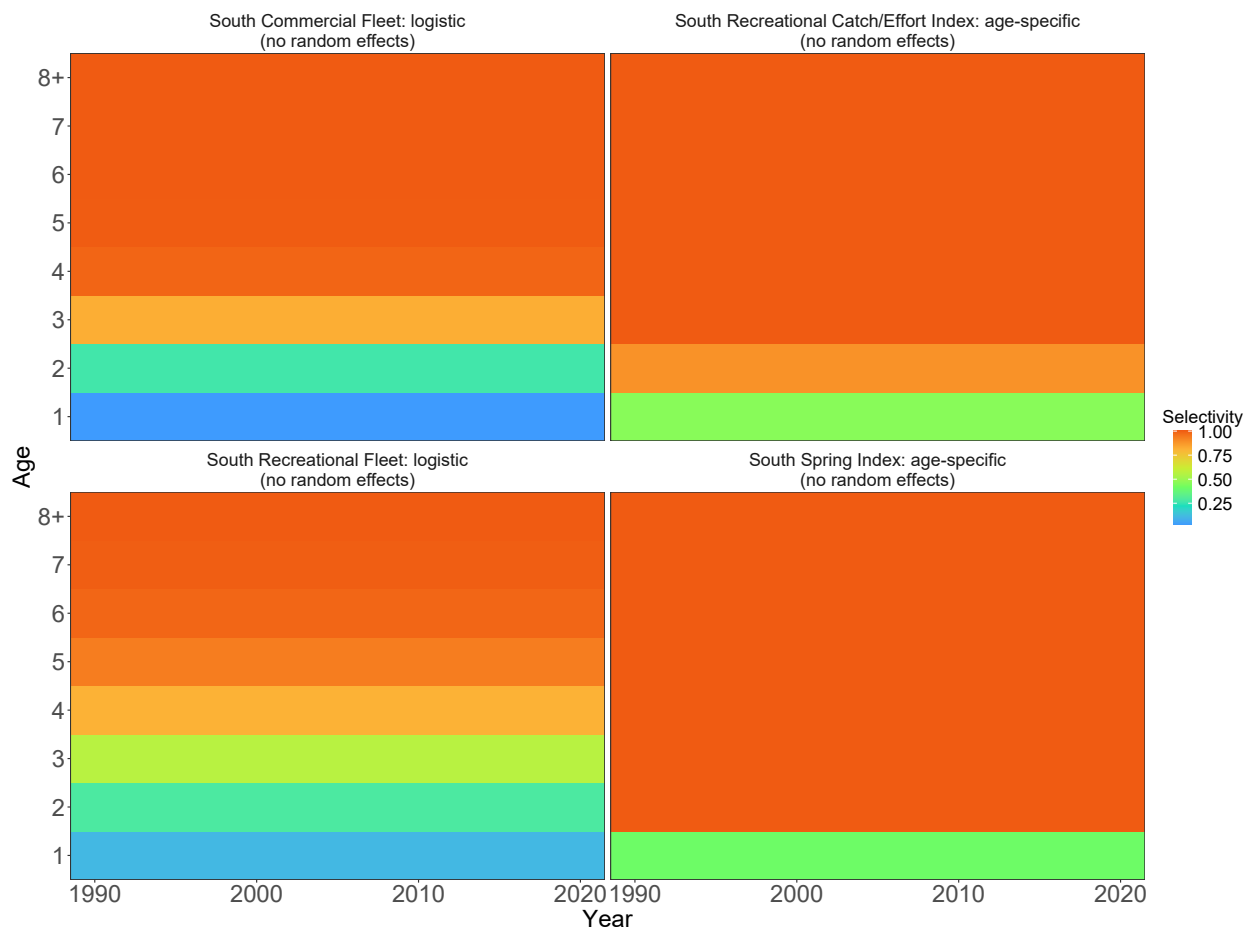


Figure S8: Selectivity for fleets and indices in the southern region.

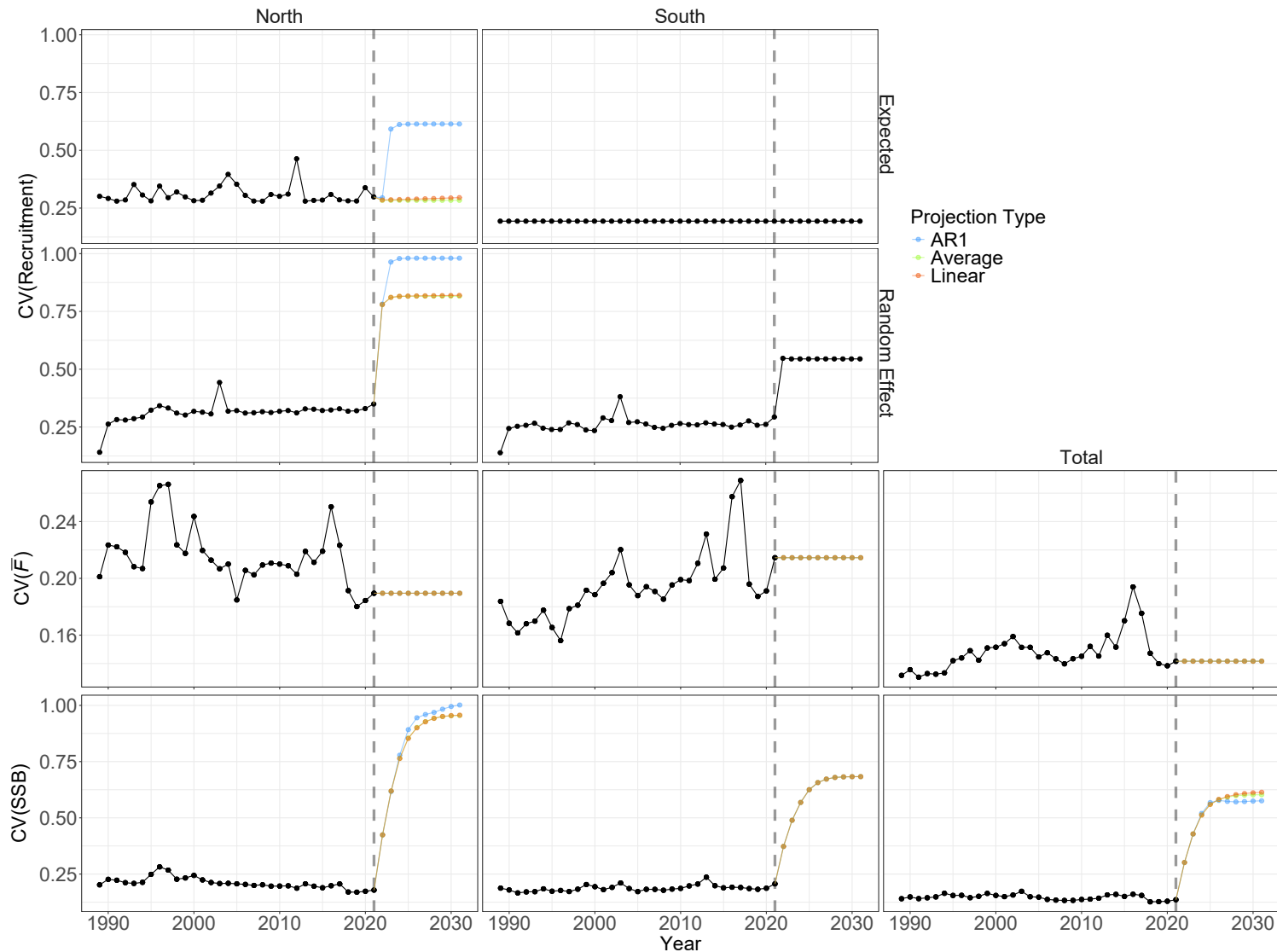


Figure S9: Coefficients of variation for estimates of alternative recruitment estimates (random effects or expected), average fishing mortality at age 6 and 7, and SSB by region and in total from model M_1 . Values in years after 2021 are from projecting model M_1 under three alternative assumptions for the bottom temperature anomalies.

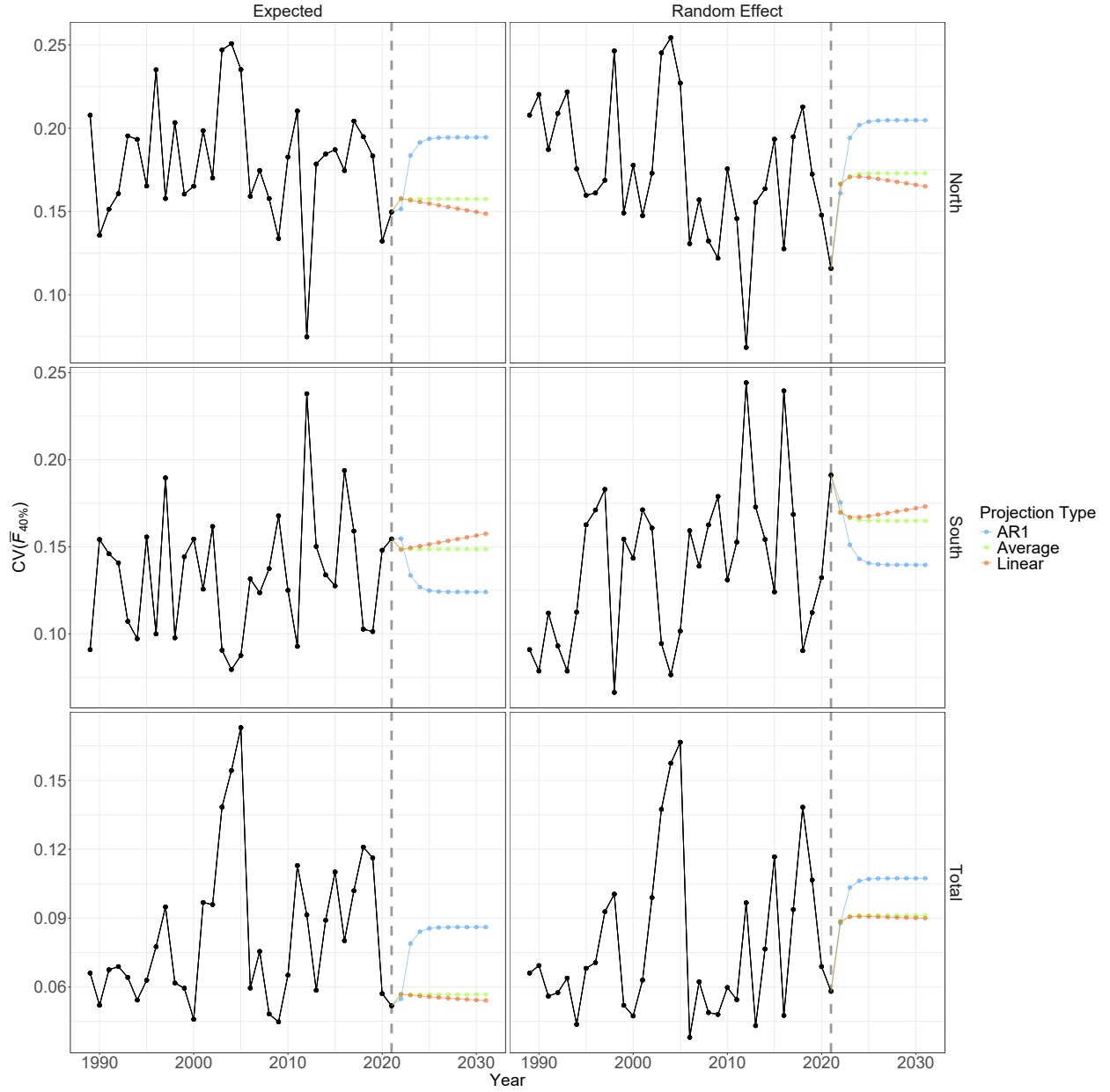


Figure S10: Coefficients of variation for annual equilibrium average F at ages 6 and 7 that produces the 40% spawning potential ratio as a function of annual expected recruitment or recruitment random effects and annual inputs to $\phi(\bar{F})$ calculations. Estimates in years after 2021 are from projecting model M_1 under three alternative assumptions for the bottom temperature anomalies.

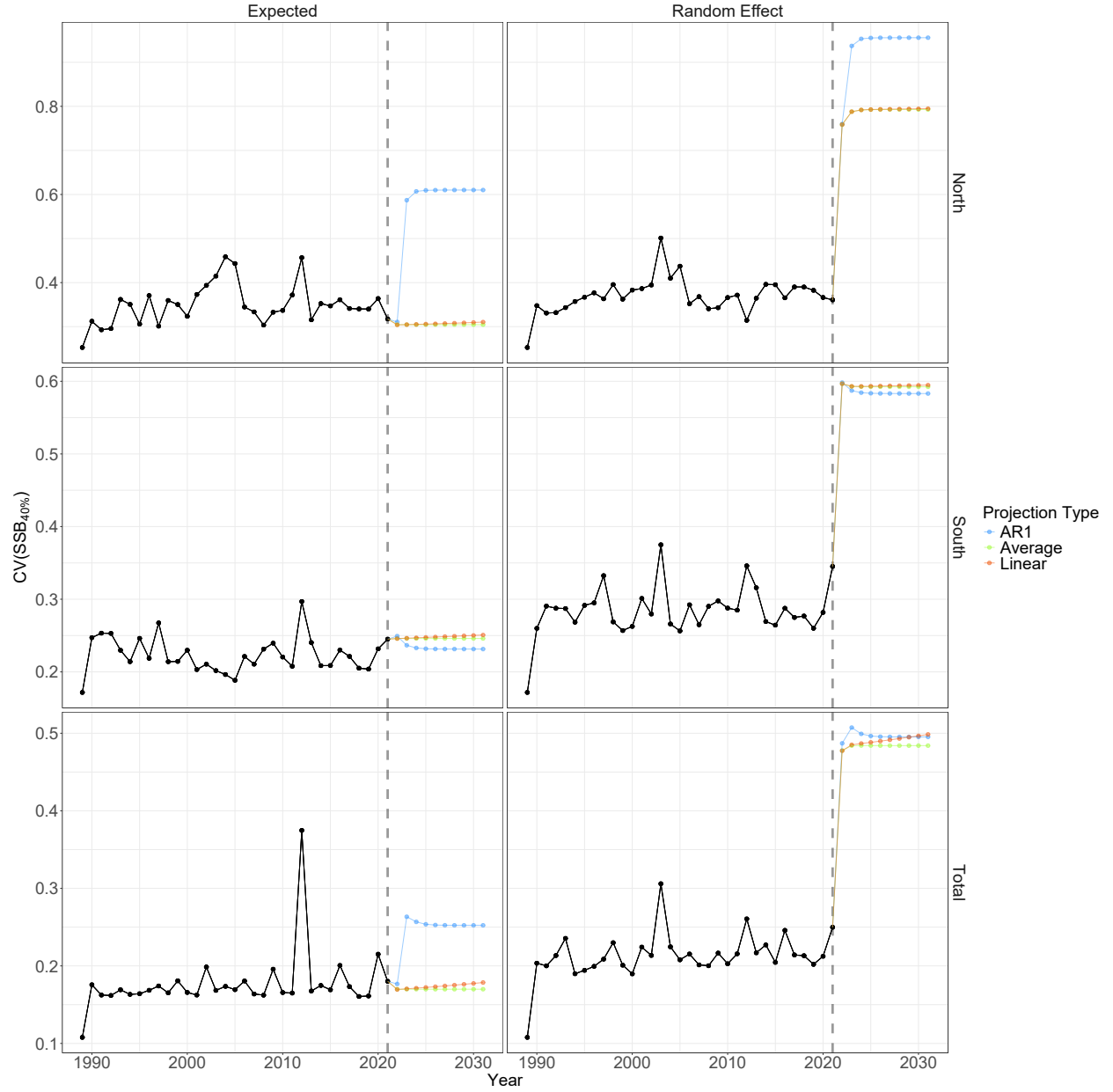


Figure S11: Coefficients of variation for annual equilibrium $SSB_{40\%}$ as a function of annual expected recruitment or recruitment random effects and annual inputs to $\phi(F)$ calculations and alternative annual recruitment types. Estimates in years after 2021 are from projecting model M_1 under three alternative assumptions for the bottom temperature anomalies.

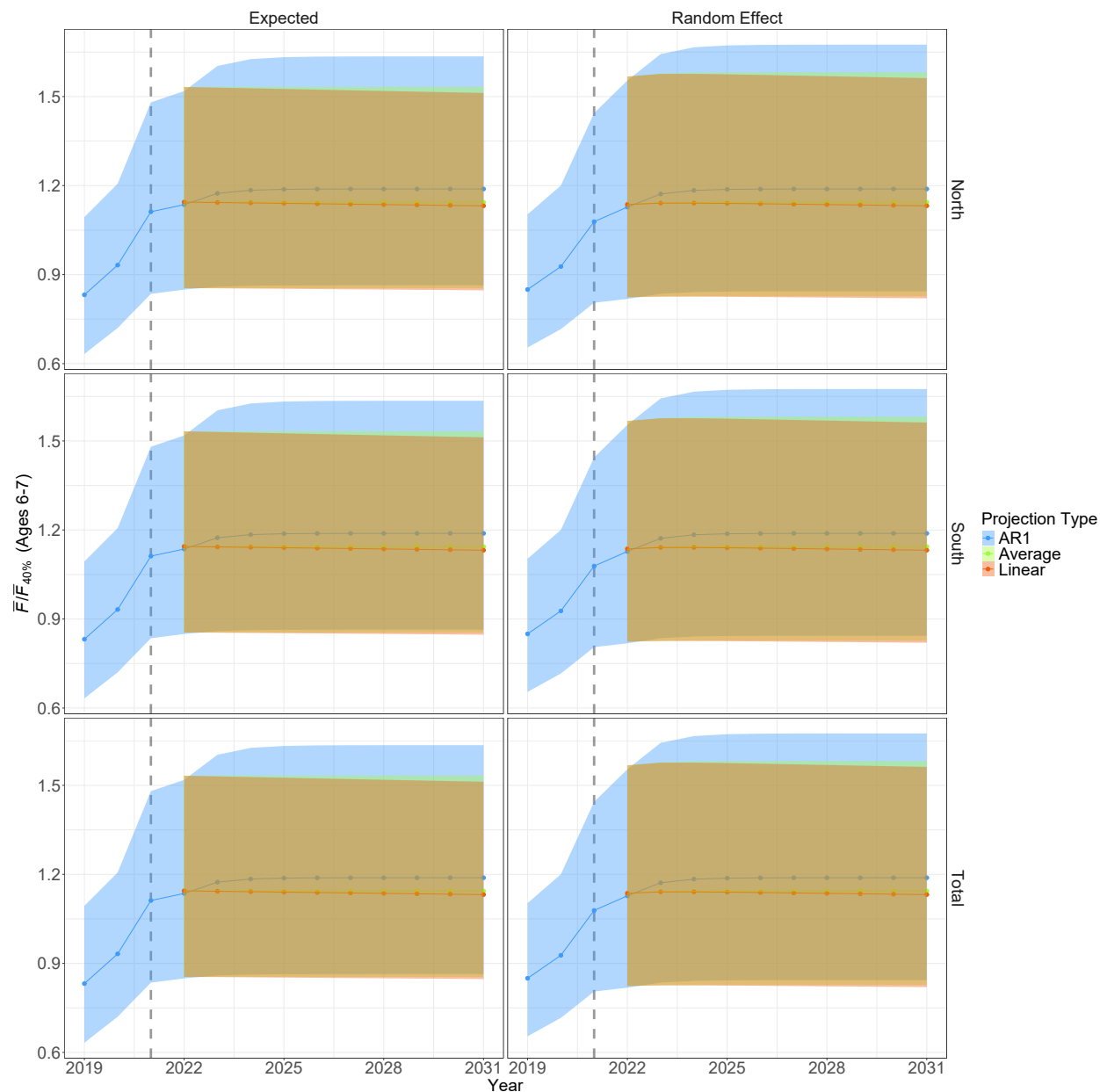


Figure S12: Annual estimates of ratios of fishing mortality to $F_{40\%}$ by region and in total. Estimates in years beyond 2021 are from projecting model M_1 under alternative assumptions for bottom temperature anomalies in the northern region. Vertical dotted line is the last year of data and polygons represent 95% confidence intervals.

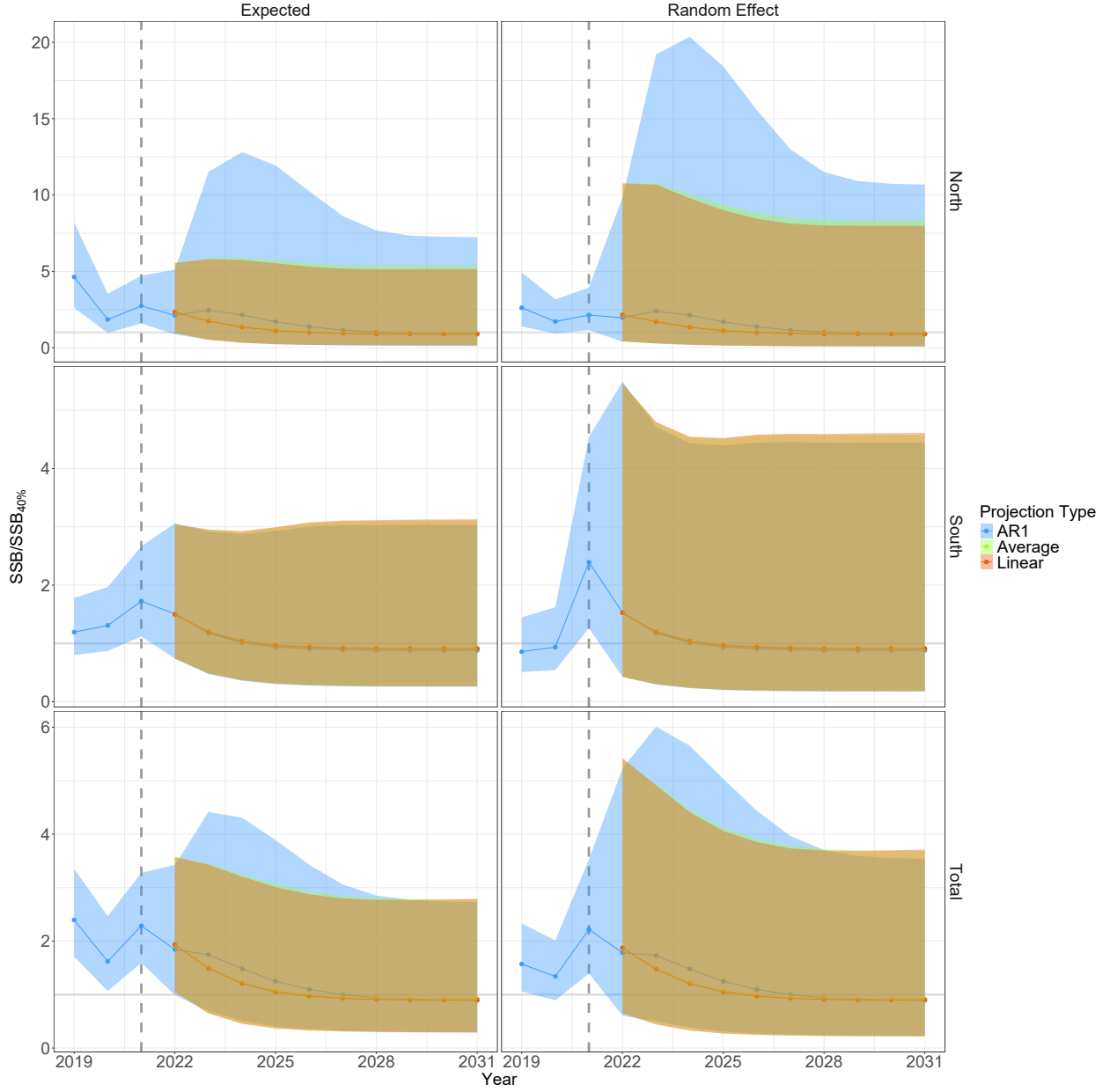


Figure S13: Annual estimates of ratios of SSB to $SSB_{40\%}$ by region and in total. Estimates in years beyond 2021 are from projecting model M_1 under alternative assumptions for bottom temperature anomalies in the northern region. Vertical dotted line is the last year of data and polygons represent 95% confidence intervals.

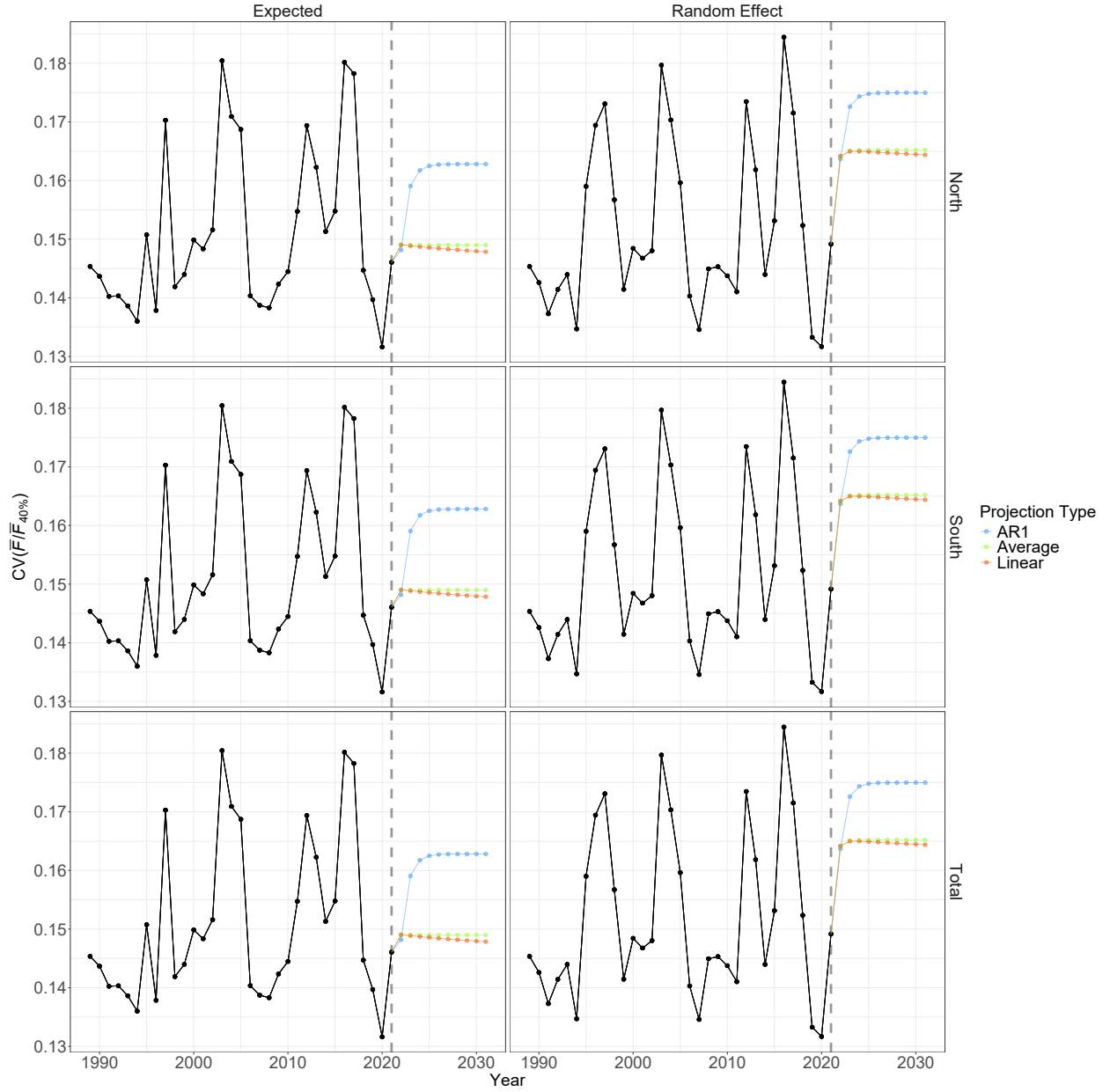


Figure S14: Coefficients of variation for annual ratios of average fishing mortality and equilibrium $\bar{F}_{40\%}$ at ages 6 and 7 where the latter is a function of annual expected recruitment or recruitment random effects and annual inputs to $\phi(\bar{F})$ calculations. Estimates in years after 2021 are from projecting model M_1 under three alternative assumptions for the bottom temperature anomalies.

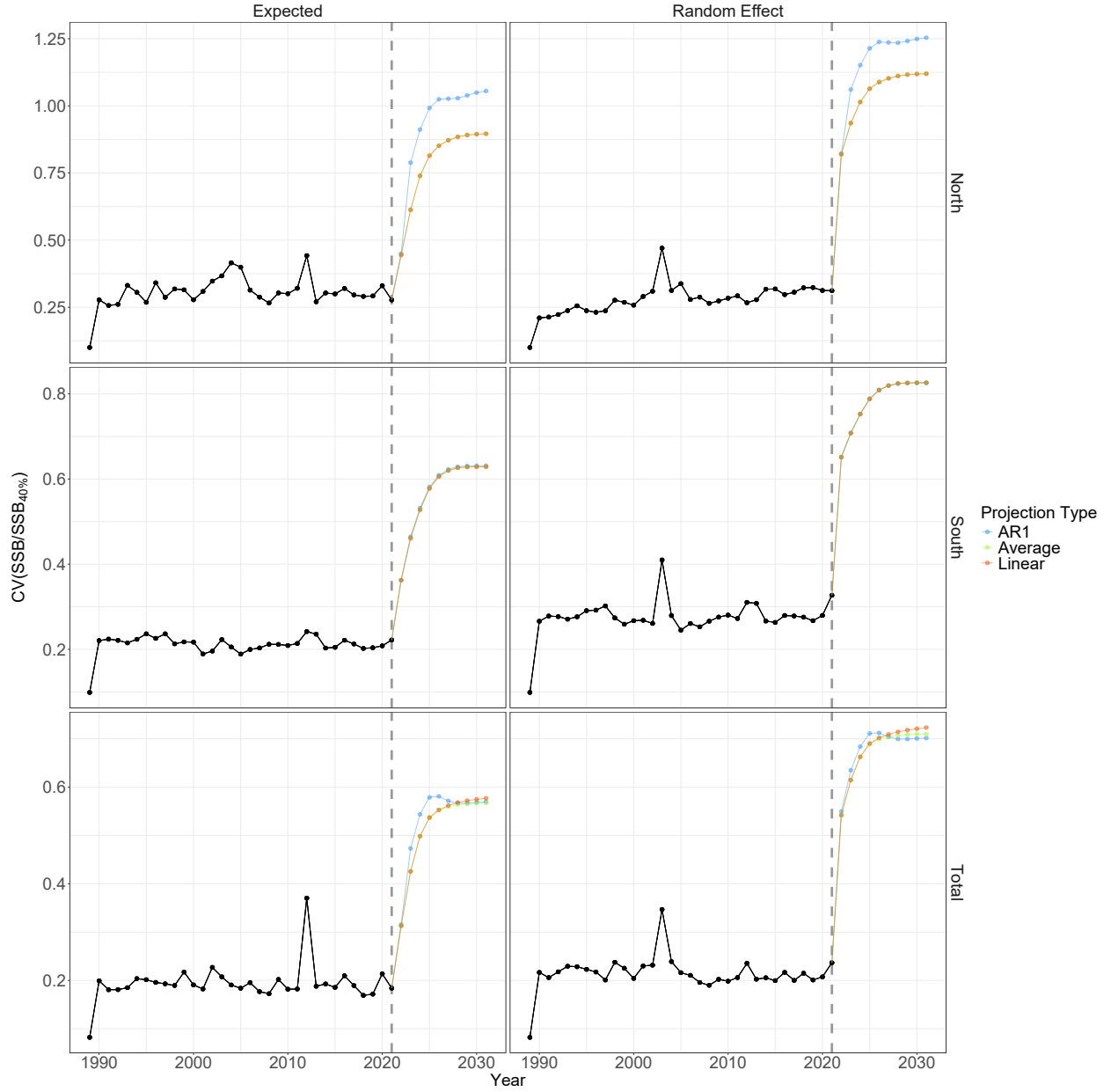


Figure S15: Coefficients of variation for annual ratios of SSB and equilibrium SSB_{40%} where the latter is a function of annual expected recruitment or recruitment random effects and annual inputs to $\phi(\bar{F})$ calculations. Estimates in years after 2021 are from projecting model M_1 under three alternative assumptions for the bottom temperature anomalies.

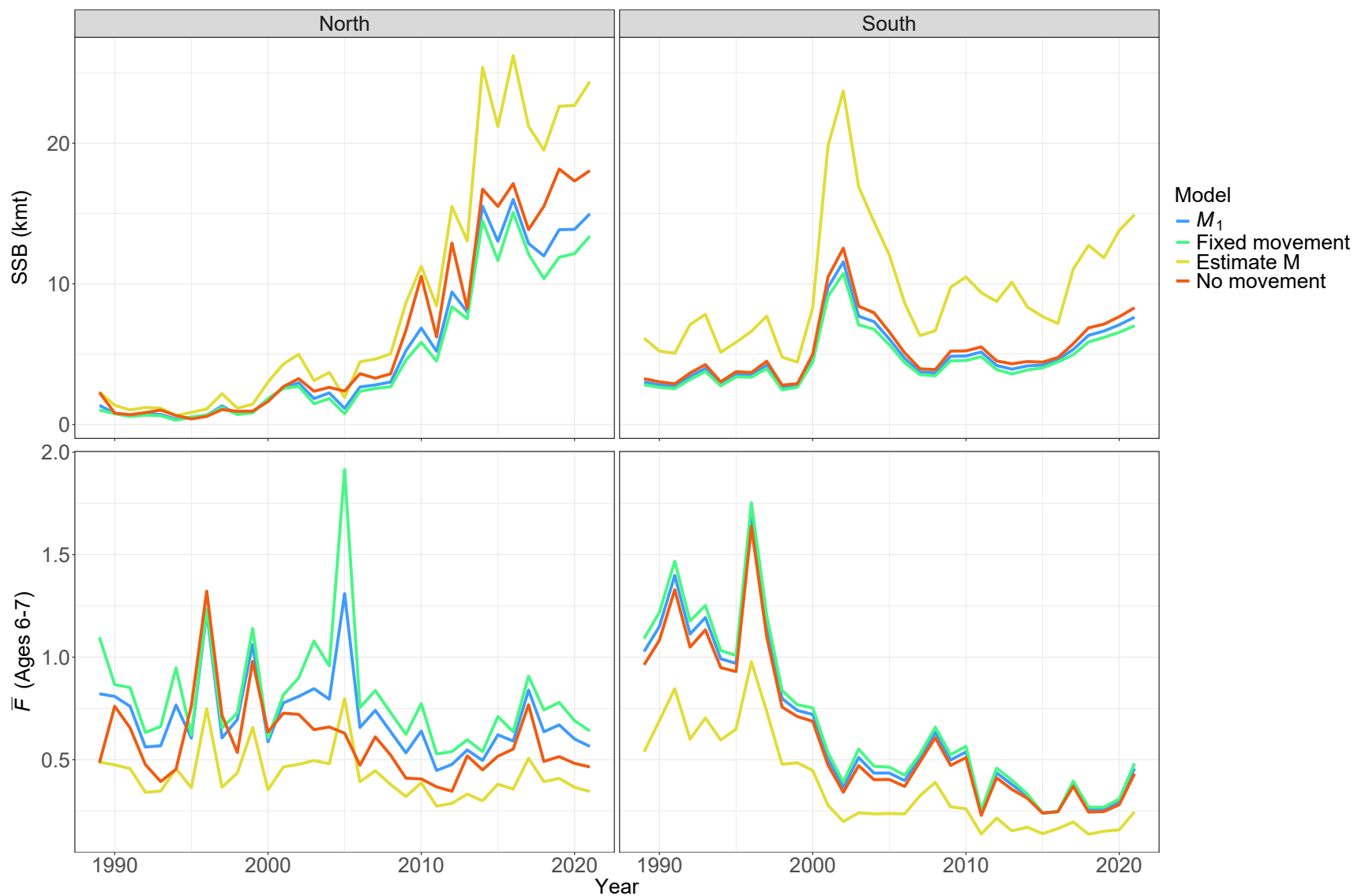


Figure S16: Estimates of annual SSB and fishing mortality rates for the best performing model M_1 and models that are otherwise the same except where 1) movement rates are fixed at the means for the prior distribution, 2) a constant natural mortality rate is estimated, or 3) there is no movement for either stock component.